AWARD NUMBER: **W81XWH-19-1-0463**

TITLE: Biodegradable Cationic Nanoparticles as a Push Chemodrug Carrier and a Pull cfDNA Scavenger Against Breast Cancer Metastasis

PRINCIPAL INVESTIGATOR: **Kam W. LEONG**

CONTRACTING ORGANIZATION: **Columbia University Medical Center (CUMC)**
New York, NY

REPORT DATE: **August 2022**

TYPE OF REPORT: **Annual**

PREPARED FOR: **U.S. Army Medical Research and Development Command**
Fort Detrick, Maryland 21702-5012

REPORT DOCUMENTATION PAGE

Form Approved
OMB No. 0704-0188

1. REPORT DATE	2. REPORT TYPE	3. DATES COVERED
August 2022	Annual	15Jul2021-14Jul2022

4. TITLE AND SUBTITLE

Biodegradable Cationic Nanoparticles as a Push Chemodrug Carrier and a Pull cfDNA Scavenger Against Breast Cancer Metastasis

5a. CONTRACT NUMBER
W81XWH-19-1-0463

5b. GRANT NUMBER
BC180904

5c. PROGRAM ELEMENT NUMBER

6. AUTHOR(S)

Kam LEONG
e-mail: kwl2121@columbia.edu

5d. PROJECT NUMBER

5e. TASK NUMBER

5f. WORK UNIT NUMBER

7. PERFORMING ORGANIZATION NAME(S) AND ADDRESS(ES)

Columbia University Medical Center
Lasker Building - Rm 450C
3960 Broadway
New York, NY 10032 (USA)

8. PERFORMING ORGANIZATION REPORT NUMBER

9. SPONSORING / MONITORING AGENCY NAME(S) AND ADDRESS(ES)

U.S. Army Medical Research and Development Command (USAMRDC)
Fort Detrick, Maryland 21702-5012

10. SPONSOR/MONITOR'S ACRONYM(S)

11. SPONSOR/MONITOR'S REPORT

12. DISTRIBUTION / AVAILABILITY STATEMENT
Approved for Public Release; Distribution Unlimited

13. SUPPLEMENTARY NOTES

14. ABSTRACT

The goal of this project is to develop a novel therapeutic approach for the prevention of breast cancer metastasis, by using *nucleic acid binding nanoparticles* (NABNPs) designed to deliver high payloads of cytotoxic drugs to tumor tissues, while simultaneously scavenging the pro-inflammatory *cell-free DNA* (cfDNA) that is released in the blood circulation as a result of tumor progression and/or destruction by chemotherapy. It is well established that cfDNA released by apoptotic and necrotic cancer cells acts as *damage-associated molecular pattern* (DAMP) molecule, and displays pro-invasive and pro-metastatic activity on breast cancer cells by activating *Toll-like receptors* (TLRs), therefore representing a promising pharmacological target for the development of anti-tumor treatments against breast cancer. In this study, we propose to develop bio-compatible NABNPs that can bind and sequester cfDNA with high affinity and that, at the same time, can be "loaded" with high amounts of cytotoxic drugs used in conventional chemotherapy (taxanes, doxorubicin) and then used to preferentially deliver such drugs to tumor sites. The goal is to inhibit tumor progression at primary tumor sites by delivering high payloads of conventional chemotherapy in a selective and sustained manner, while, at the same time, inhibiting metastatic dissemination of cancer cells by scavenging cfDNA released by dying cells. The project is structured into three specific aims: 1) to synthesize and optimize NABNPs with respect to cfDNA-scavenging ability, drug delivery efficiency, and low toxicity; 2) to evaluate the anti-metastatic activity of NABNPs and investigate the cellular mechanisms that underpin it; 3) to evaluate the safety, biodistribution and therapeutic efficacy against both primary tumors and metastases of drug-loaded NABNPs in relevant *in vivo* breast cancer models, including *patient-derived xenografts* (PDX) from *triple-negative breast carcinomas* (TNBCs) that can sustain the development of spontaneous lung metastases in immune-deficient mice. This is a **collaborative research project** conducted in partnership by two research teams (Kam W. Leong, Piero Dalerba) with the support of two distinct awards **(BC180904, BC180904P1)**.

15. SUBJECT TERMS
Breast cancer, Metastasis, Chemotherapy, Drug formulation, Nanoparticles, Circulating free DNA, DNA scavenging, Anti-inflammatory effects, Prevention of metastasis

16. SECURITY CLASSIFICATION OF:			17. LIMITATION OF ABSTRACT	18. NUMBER OF PAGES	19a. NAME OF RESPONSIBLE PERSON
a. REPORT	b. ABSTRACT	c. THIS PAGE			USAMRDC
Unclassified	Unclassified	Unclassified	Unclassified	25	19b. TELEPHONE NUMBER *(include area code)*

TABLE OF CONTENTS

1. INTRODUCTION.

The goal of this project is to develop a novel therapeutic approach for the prevention of breast cancer metastasis, by using *nucleic acid binding nanoparticles* (NABNPs) designed to deliver high payloads of cytotoxic drugs to tumor sites, while simultaneously scavenging the pro-inflammatory *cell-free DNA* (cfDNA) that is released in the blood circulation as a result of tumor progression and/or destruction by chemotherapy.

2. KEYWORDS.

Breast cancer, Metastasis, Chemotherapy, Drug formulation, Nanoparticles, Circulating free DNA, DNA scavenging, Anti-inflammatory effects, Prevention of metastasis

3. ACCOMPLISHMENTS.

Major goals of the project. This is a collaborative project conducted in partnership by two research teams (Kam W. Leong, Piero Dalerba), supported by two distinct awards (BC180904, BC180904P1). The project envisions three specific aims, pursued in collaboration by the two research teams:

AIM 1: To synthesize and optimize *nucleic acid binding nanoparticles* (NABNPs) with respect to cfDNA-scavenging ability, drug delivery efficiency and low toxicity. This aim includes only one major task: **Major Task 1 [Synthesis and characterization of NABNPs]**.

AIM 2: To evaluate the anti-metastatic effect of NABNPs as cfDNA scavengers and drug carriers, as well as investigate their anti-metastatic mechanism *in vitro*. This aim includes three major tasks: **Major Task 2 [Evaluation of the capacity of taxane-loaded NABNPs to scavenge cfDNA and inhibit breast cancer cell migration *in vitro*]**, **Major Task 3 [Evaluation of the disruption of the cfDNA-related complexes and the neutralization of cfDNA-related micro-vescicles by NABNPs], Major Task 4 [Elucidation of the cfDNA-scavenger mechanism of NABNPs by tracking endocytosis and intracellular bio-distribution]**.

AIM 3: To evaluate the biodistribution and therapeutic efficacy of NABNPs using *in vivo* models of breast cancer metastasis. This aim includes six major tasks: **Major Task 5 [Regulatory approval of animal research experiments]**, **Major Task 6 [Generation and validation of animal breast cancer models for the *in vivo* study of spontaneous metastasis], Major Task 7 [Evaluation of the pharmacokinetics, biodistribution and accumulation of NABNPs *in vivo*]**, **Major Task 8 [Evaluation of therapeutic efficacy of taxane-loaded NABNPs in the 4T1 model of spontaneous metastasis]**, **Major Task 9 [Evaluation of therapeutic efficacy of taxane-loaded NABNPs in PDX models]**, **Major Task 10 [Preparation of a manuscript reporting study results]**.

Accomplishments under the goals:

Major Task 1: Synthesis and characterization of NABNPs. This major task was, for the most part, to be pursued during the 1st year of the award. Indeed, during the first three years of the award (07/15/2019-07/14/2022), the research team completed the design, chemical synthesis, biophysical and biochemical study of various types of NABNPs **(Subtasks 1.1-1.4).**

Design, chemical synthesis and functional characterization of NABNPs. *Polyamidoamine* (PAMAM) is a biodegradable, hyperbranched, spherically-shaped polymer that can be cationic, neutral or anionic depending on whether it contains amino-, hydroxyl-, or carboxyl-functionalized terminal branches, respectively. Preliminary data from our laboratory, as well as recent publications from other investigators revealed that cationic, amine-terminated PAMAM has strong affinity for DNA. Recently, Ibtehaj *et al.* (*Molecular Therapy*, 26:1020-1031, 2018) demonstrated that 3rd generation, soluble poly-amidoamine dendrimers (PAMAM-G_3) can decrease *Tool-like Receptor 9* (TLR9) activation by scavenging cfDNA in blood, thus resulting in a dramatic reduction in liver metastases in a murine model of pancreatic cancer. Unfortunately, this treatment based on PAMAM-G_3 only succeeded in suppressing metastatic cancer and did not inhibit primary cancer progression. This led us to hypothesize that the

cfDNA scavenging properties of PAMAM-G3 could be combined with standard chemotherapy treatment, in order to achieve, at the same time, control of primary tumor growth and inhibition of metastatic spread caused by treatment-induced release of cfDNA. We therefore proceeded to design **(Subtask 1.1)**, synthesize **(Subtask 1.2)** and functionally characterize **(Subtasks 1.3-1.5)** a library of distinct PAMAM polymers with varying degrees of tertiary amine conjugation or hydrophobic alkyl (C12) chain derivatization **(Table 1, Figure 1A)**.

	Name	Number of Terminal Groups	Grafting Groups	Number of Grafting	% of Grafting	MW (Da)	DNA binding EC_{50} (Polymer: DNA)	Toxicity IC_{50} ($\mu g\ mL^{-1}$)
1	G3-NH_2	32	-	0	0	6910	0.67	31.6
2	G3-$DMEA_{24}$	32	DMEA	24	75.0%	9210	1.00	>500
3	G3-$DEEA_{10}$	32	DEEA	10	31.2%	8340	0.52	>500
4	G3-$DEEA_{24}$	32	DEEA	24	75.0%	9770	1.10	>500
5	G4-NH_2	64	-	0	0	14220	0.71	11.7
6	G4-$DMEA_{40}$	64	DMEA	40	62.5%	18820	1.04	>500
7	G4-$DMEA_{50}$	64	DEMA	50	78.1%	19970	0.83	>500
8	G4-$DEEA_{21}$	64	DEEA	21	32.8%	17220	0.83	19.5
9	G4-$DEEA_{40}$	64	DEEA	40	62.5%	19940	1.21	>500
10	G4-$DEEA_{50}$	64	DEEA	50	78.1%	21370	0.54	>500
11	G4-$DBEA_{20}$	64	DBEA	20	31.2%	18200	>10	50.5
12	G4-$DBEA_{40}$	64	DBEA	40	62.5%	21980	9.7	166.9
13	G2.5-COOH	32	-	0	0	6270	>10	>500
14	G3.5-COOH	64	-	0	0	12930	>10	>500

Table 1. Chemical structure and biological properties of PAMAM polymers selected for study. DMEA: dimethyl-ethanolamine; DEEA: diethyl-ethanolamine; DBEA: dibutyl-ethanolamine; MW: molecular weight.

One of the major challenges associated with the use of PAMAM dendrimers as biomaterials is their high density of surface amino groups, which confer them a highly positive surface electrical charge, a feature that associates with cytotoxicity, but is also key to their beneficial cfDNA scavenging ability. To solve this issue, and try *"dissecting"* cell cytotoxicity from cfDNA scavenging ability, we modified the surface amino groups with N,N-dialkyl-ethanolamine by esterification **(Figure 1A)**. In this way, a portion of the surface amino groups were shielded, without substantially modifying the overall positive charge of NABNPs. A series of PAMAM-G3 and PAMAM-G4 derivatives were synthesized, by modification of surface amino groups using dimethyl-, diethyl-, and dibutyl-ethanolamines (DMEA, DEEA, DBEA) **(Table 1, Fig. 1A)**. In order to identify the PAMAM polymers best suited for *in vivo* applications, we conducted a systematic study of their biophysical and biological properties, with a special focus on their capacity to scavenge cfDNA (expressed as EC_{50}), intrinsic cytotoxicity on *in vitro* cultured cells (expressed as IC_{50}) and capacity to inhibit the activation of three independent TLRs (TLR3, TLR8, TLR9) know to be activated by nucleic acids **(Table 1, Fig. 1B)**. Our results showed that cationic PAMAM dendrimers with unmodified -NH2 groups exhibited strong DNA scavenging ability, but also displayed high toxicity. Anionic PAMAM dendrimers with -COOH groups exhibited low toxicity, but showed weak DNA scavenging ability. Surface modification using DBEA resulted in reduced scavenging ability and higher cytotoxicity. On the other hand, surface modification using DEEA appeared to associate with lower cytotoxicity, while retaining good DNA binding ability, resulting in efficient inhibition of all three TLRs (TLR3, TLR8, TLR9).

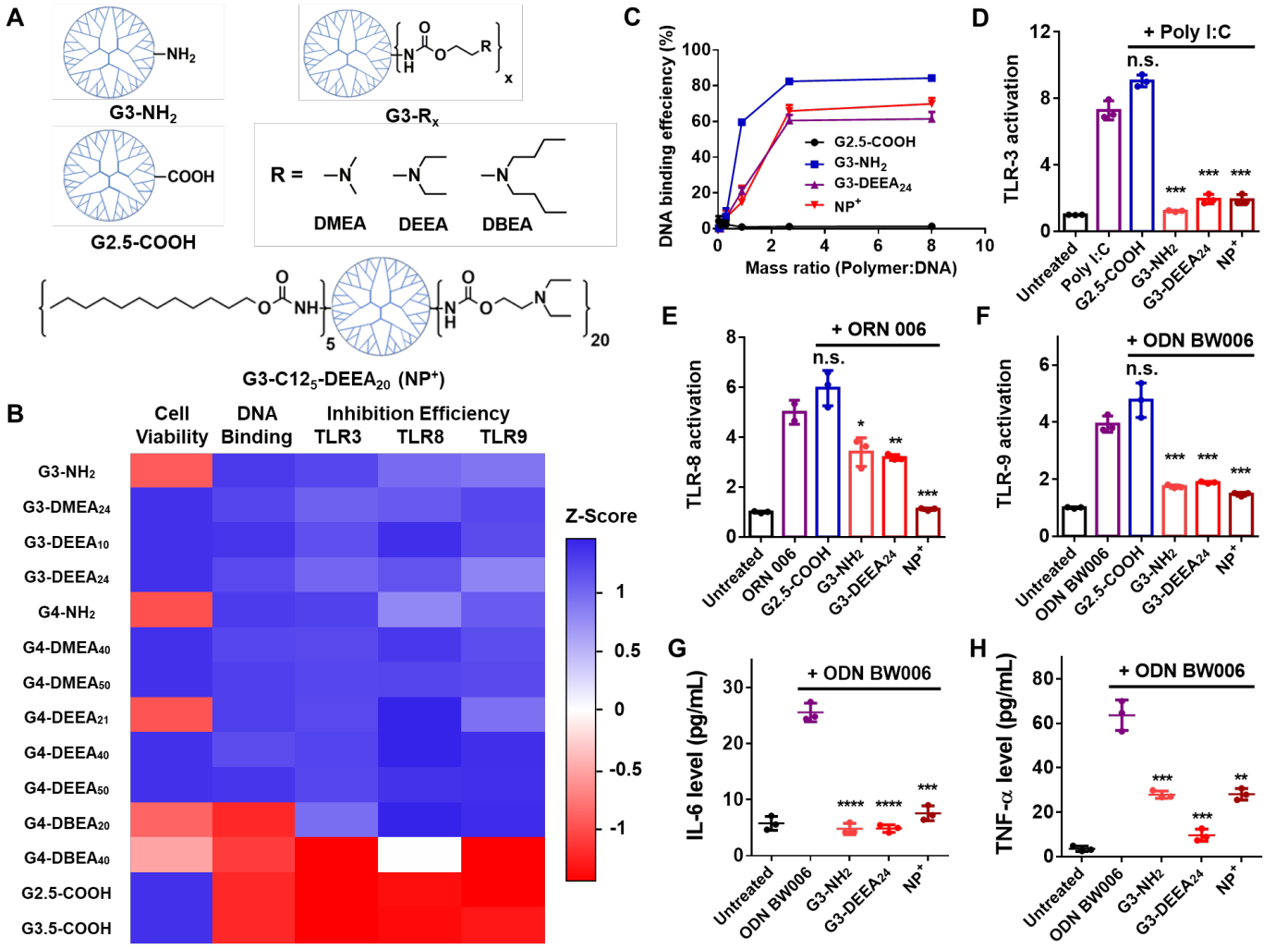

Figure 1. Structural and biological properties of PAMAM polymers selected for study. (A) Chemical structure of PAMAM derivatives and the optimized G3-C12$_5$-DEEA$_{20}$ dendrimer formulation. **(B)** Evaluation of PAMAM derivatives with regard to cell cytotoxicity, DNA scavenging capacity and inhibitory properties towards TLR signaling. Results are normalized to Z-scores. **(C)** DNA binding efficiency of different PAMAM polymers across polymer/DNA mass ratios. **(D-F)** Inhibitory effects of different PAMAM polymers on the activation of TLR3 (D), TLR8 (E) and TLR9 (F) signaling in HEK-Blue-hTLR reporter cells stimulated with corresponding nucleic-acid agonists. **(G-H)** Inhibitory effects of different PAMAM polymers on the secretion of IL-6 (G) and TNFα (H) by Raw264.7 macrophage cells treated with the TLR9 agonist ODN-BW006. Statistical significance was calculated using Student's t test. Data were compared to the agonist group unless indicated otherwise. *P<0.05, **P<0.01, ***P<0.001, ****P<0.0001 (Student's t-test). Error bars: mean ± SD.

	Name	Number of Terminal Groups	Grafting Groups	Number of Grafting	% of Grafting	MW (Da)	Diameter (nm)	Zeta potential (mV)
15	NP (G3-C12$_5$-DEEA$_{20}$)	32	DEEA&C12	25	78.1%	10280	141.8±3.3	58.2±4.8
16	NP (G3-C12$_9$-DEEA$_{20}$)	32	DEEA&C12	29	90.6%	11140	186.8±5.6	55.0±0.6
17	NP (G4-C12$_7$-DEEA$_{35}$)	64	DEEA&C12	42	65.6%	19310	172.6±0.4	62.6±1.6
18	NP (G4-C12$_9$-DEEA$_{35}$)	64	DEEA&C12	44	68.8%	20170	194.5±2.4	60.8±2.1
19	NP (G4-C12$_{15}$-DEEA$_{35}$)	64	DEEA&C12	50	78.1%	21450	164.0±9.5	65.4±2.1

Table 2. Chemical and physical properties of the second set of PAMAM-DEEA polymers selected for the study.

Based on the results of our first screen, we selected PAMAM-G3-DEEA$_{24}$ and PAMAM-G4-DEEA$_{40}$ as top candidates for further study, as they displayed low cytotoxicity, good DNA-binding capacity and high ability to inhibit the activation of TLR3, TLR8 and TLR9. As a next step, we modified the hydrophilic dendrimers with dodecyl groups, in order to confer amphiphilicity, using different ratios of dodecyl groups, and then compared the hydrodynamic diameters and electrical charges (zeta potentials) of the resulting NABNPs **(Table 2)**. Overall, all derivatives displayed similar properties. Based on the results of this second screen, we chose the PAMAM-G3-C12$_5$-DEEA$_{20}$ nanoparticle formulation (NP$^+$) as our lead candidate, especially because of its smaller size (141.8±3.3 nm), which was expected to allow for increased bio-distribution to tumor tissues and improved cellular uptake.

Major Task 2: Evaluation of the capacity of taxane-loaded NABNPs to scavenge cfDNA and inhibit breast cancer cell migration *in vitro*. During the three years of the award, our research teams completed a large array of joint experiments, aimed at testing the capacity of the lead NABNP candidate (PAMAM-G3-C12$_5$-DEEA$_{20}$) to carry high payloads of the anti-tumor agent *paclitaxel* (PTX), scavenge cfDNA *in vitro*, inhibit TLR activation as well as inhibit the proliferation and *in vitro* migration of breast cancer cells **(Subtasks 2.1-2.3)**.

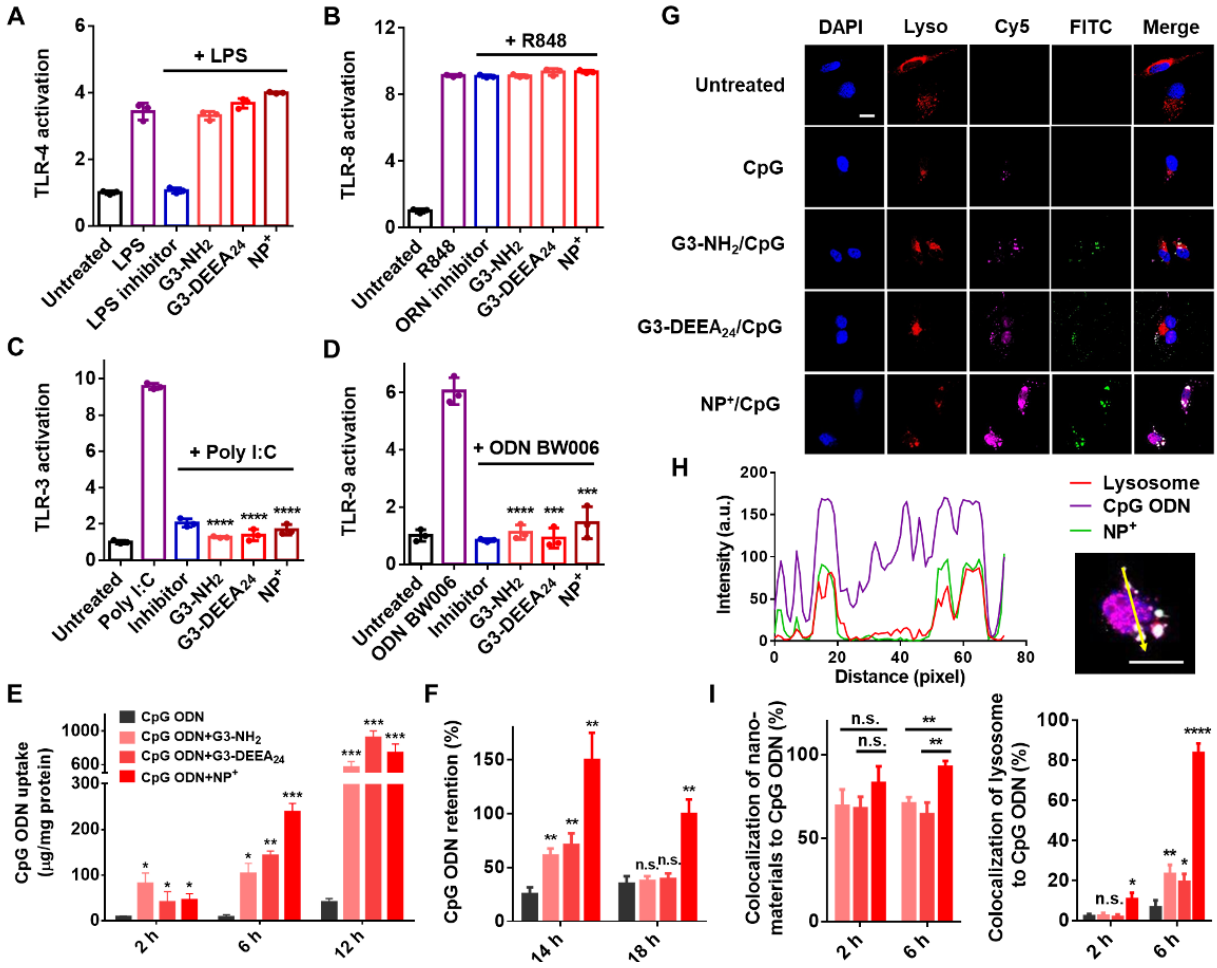

Figure 2. TLR inhibition and intracellular trafficking of cationic nanomaterials. (A-B) TLR4 (A) and TLR8 (B) activation assays showing that cationic NABNPs are unable to inhibit TLR activation induced by non-NA agonists. Results are normalized to untreated groups. The mass ratio of NABNPs to agonists was 10:1. **(C-D)** TLR3 (C) and TLR9 (D) activation assays where cationic NABNPs were added to cell cultures for 2 hours and then removed immediately before stimulation with agonists. Results are normalized to untreated groups and tested for difference with the agonist group. **(E-F)** Cellular uptake (E) and retention (F) of CpG-ODNs in either presence or absence of cationic NABNPs. CpG-ODNs were labeled with Cy5. **(G)** Imaging by fluorescence microscopy of MDA-MB-231 cells, showing cellular uptake of CpG-ODNs and cationic NABNPs after 6 hours of incubation (DAPI: cell nuclei; LysoTracker-Red: lysosomes; Cy5: CpG-ODNs; FITC: cationic NABNPs). Scale bar: 20 μm. **(H)** Colocalization profiles of CpG-ODNs, PAMAM-G3-C12$_5$-DEEA$_{20}$ NABNPs (NP$^+$) and lysosomes along the direction of the yellow arrow in the image of the nucleus with merged colors. Scale bar: 20 μm. **(I)** Quantification of colocalization percentages using *Mander's overlap coefficient* (MOC). Results are normalized to CpG-ODN groups at same time points unless indicated otherwise. Statistical significance was calculated using Student's t test. *P<0.05, **P<0.01, ***P<0.001, ****P<0.0001. Error bars: mean ± SD.

Evaluation of the capacity of PAMAM-G3-C12$_5$-DEEA$_{20}$ NABNPs (NP$^+$) to scavenge cfDNA and inhibit TLR activation. As a first step, we compared the functional properties of PAMAM-G3-C12$_5$-DEEA$_{20}$ NABNPs (NP$^+$) to those of other PAMAM dendrimers, with regard to their capacity to scavenge cfDNA *in vitro* **(Subtask 2.1)** and inhibit TLR signaling **(Subtask 2.2)**. As compared to other cationic dendrimers, PAMAM-G3-C12$_5$-DEEA$_{20}$ NABNPs (NP$^+$) showed similar DNA binding ability, resulting in efficient inhibition of TLR3, TLR8, and TLR9 activation **(Figure 1C-F)**, as well as suppression of TNFα and IL-6 secretion by RAW264.7 murine macrophages following stimulation with CpG oligodeoxy-nucleotides (CpG-ODNs) **(Figure 1G-H).** The inhibitory effect of PAMAM-G3-C12$_5$-DEEA$_{20}$ NABNPs (NP$^+$) appeared selective to TLRs activated by *nucleic acids* (NAs), as it was not observed when reporter cells were stimulated with *lipopolysaccharide* (LPS) to activate TLR4 **(Figure 2A)**, and also appeared mediated by NA scavenging, as it was not observed when reporter cells were stimulated with R848, a non-NA agonist of TLR8 **(Figure 2B).**

Evaluation of the capacity of PAMAM-G3-C12$_5$-DEEA$_{20}$ NABNPs (NP$^+$) to inhibit breast cancer cell migration *in vitro* and deliver equivalent payloads of cytotoxic chemotherapy. We also evaluated the capacity of PAMAM-G3-C12$_5$-DEEA$_{20}$ NABNPs (NP$^+$) to inhibit the proliferation and *in vitro* migration of breast cancer cells following exposure to *damage-associated molecular pattern* (DAMP) molecules released by tumor cells following treatment with chemotherapy **(Subtask 2.3)**. To this end, we cultured human MDA-MB-231 cells onto a Matrigel-coated porous membrane and then exposed them to the tissue-culture supernatants of companion MDA-MB-231 cells treated with *paclitaxel* (PTX; 100 nM, 6 hours), either alone or in combination with various NABNP formulations (25 ug/ml). After 24 hours, we visualized the cells that had migrated through the porous membrane using a crystal violet stain, and then counted them **(Figure 3)**. Indeed, our results revealed that co-treatment with cationic NABNPs, including PAMAM-G3-C12$_5$-DEEA$_{20}$ NABNPs (NP$^+$), was able to substantially reduce MDA-MB-231 cell migration induced by exposure to supernatants of cells treated with PTX (which are known to be enriched in DAMPs such as cfDNA).

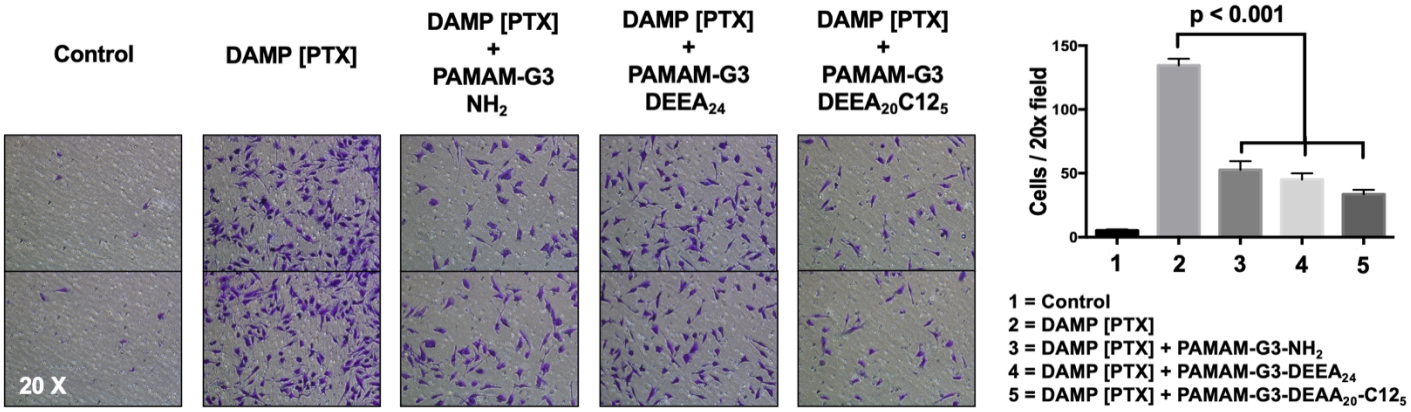

Figure 3. Evaluation of cationic NABNPs as "dampeners" of the cell motility stimulated by *damage-associated molecular pattern* (DAMP) molecules released by tumor cells following chemotherapy. MDA-MB-231 cells were cultured onto a Matrigel-coated porous membrane and exposed to tissue culture supernatants of MDA-MB-231 cells treated with paclitaxel (PTX; 100 nM, 6 hours), either alone or in combination with various cationic NABNP formulations (25 ug/ml). After 24 hours, cells migrated through the porous membrane were visualized using crystal violet and counted.

We then wanted to understand whether PAMAM-G3-C12$_5$-DEEA$_{20}$ NABNPs (NP$^+$) could be *"pre-loaded"* with cytotoxic drugs and then used as *"trojan horses"*, to deliver high payloads of the same drugs to cancer cells. To this end, we pre-loaded PAMAM-G3-C12$_5$-DEEA$_{20}$ NABNPs (NP$^+$) with different amounts of cytotoxic drugs used in the chemotherapy of breast cancer, such as PTX and *doxorubicin* (DOX), and then tested whether they were able to exert similar cytotoxic activity against MDA-MB-231 cells *in vitro*, while simultaneously retaining their ability to scavenge cell-free nucleic acids, such as cfDNA and *cell-free RNA* (cfRNA). The results of these *in vitro* experiments showed that, indeed, PAMAM-G3-C12$_5$-DEEA$_{20}$ NABNPs (NP$^+$) loaded with chemotherapy drugs have equal (if not superior) anti-tumor activity as compared to equimolar doses of chemotherapy drugs alone, and that pre-loading with cytotoxic drugs does not impair their cfDNA scavenging ability **(Figure 4)**.

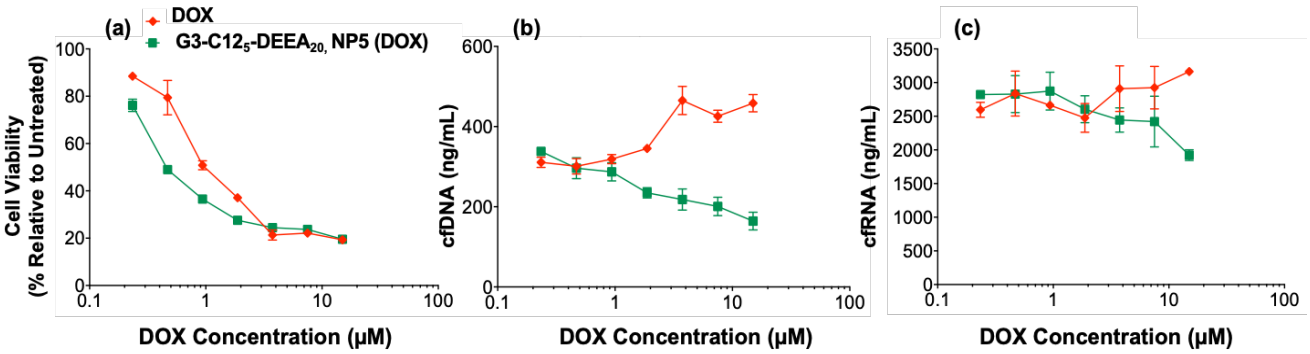

Figure 4. Comparative evaluation of the anti-tumor activity and DNA-scavenging properties of NABNPs loaded with cytotoxic drugs. (A) PAMAM-G3-C12$_5$-DEEA$_{20}$ NABNPs (NP5) loaded with doxorubicin (DOX) display similar, if not superior anti-tumor activity against MDA-MB-231 cells as compared to equimolar doses of DOX alone, as demonstrated by a lower IC$_{50}$ (i.e. a lower value for the DOX concentration necessary to achieve a 50% inhibition of tumor growth). **(B-C)** PAMAM-G3-C12$_5$-DEEA$_{20}$ NABNPs (NP5) loaded with doxorubicin (DOX) reduce *cell-free DNA* (cfDNA) and *cell-free RNA* (cfRNA) content in tissue culture supernatants of MDA-MB-231 cells treated with DOX.

Major Task 3: Evaluation of the capacity of NABNPs to disrupt cfDNA-related complexes and neutralize cfDNA-related micro-vescicles. This major task was delayed and is to be pursued during the 4th year of the award, during the *no-cost extension* (NCE) period (months: 36-48).

Major Task 4: To elucidate the cfDNA-scavenger mechanism of PAMAM-G3-C12$_5$-DEEA$_{20}$ NABNPs (NP$^+$) by tracking endocytosis and intracellular distribution of both cfDNA and NABNPs. During the first three years of the award (07/15/2019-07/14/2022), we conducted a series of experiments aimed at elucidating whether endocytosis of PAMAM-G3-C12$_5$-DEEA$_{20}$ NABNPs (NP$^+$) would be able to contribute to the intra-cellular scavenging of cfDNA and suppression of pro-inflammatory TLR signaling **(Subtasks 4.1-4.3)**.

Evaluation of the capacity of PAMAM-G3-C12$_5$-DEEA$_{20}$ NABNPs (NP$^+$) to suppress cfDNA-induced stimulation of TLR signaling by intra-cellular sequestration of cfDNA. As a first step, we evaluated whether *in vitro* pre-incubation (2 hours) with PAMAM-G3-C12$_5$-DEEA$_{20}$ NABNPs (NP$^+$) would render cells resistant to stimulation with nucleic acid species able to activate TLR3/TLR9 signaling, even after removal of PAMAM-G3-C12$_5$-DEEA$_{20}$ NABNPs (NP$^+$) from cell supernatants immediately before exposure to nucleic acids. Indeed, when this experiment was performed using HEK293 cells engineered with TRL3 and TLR9 reporters, pre-incubation with PAMAM-G3-C12$_5$-DEEA$_{20}$ NABNPs (NP$^+$) abolished TLR3 and TLR9 activation by the corresponding DAMP agonists **(Figure 2C-D)**. As a second step, we then tested whether such suppression of TLR3/TLR9 activation was associated with intra-cellular sequestration of *nucleic acids* (NAs), such as CpG *oligo-nucleotides* (ODNs). We thus incubated human MDA-MB-231 *triple-negative breast cancer* (TNBC) cells with CpG-ODNs labeled with a fluorochrome (Cy5) for 12 hours, either in the presence or absence of PAMAM-G3-C12$_5$-DEEA$_{20}$ NABNPs (NP$^+$). The results clearly showed, that co-incubation with PAMAM-G3-C12$_5$-DEEA$_{20}$ NABNPs (NP$^+$) promoted the intra-cellular accumulation of CpG-ODNs **(Figure 2E-F).** Finally, we evaluated whether co-incubation of PAMAM-G3-C12$_5$-DEEA$_{20}$ NABNPs (NP$^+$) and CpG-ODNs would lead to their co-localization and accumulation within the lysosomal system of the cell. To this end, we incubated MDA-MB-231 cells with CpG-ODNs and NABNPs conjugated with different fluorochromes (Cy5, FITC) and then stained them with dyes to visualize lysosomes (LysoTracker Red) and nuclei (DAPI). The results clearly showed that, in cells co-incubated with NABNPs, CpG-ODNs accumulated alongside NABNPs within lysosomes **(Figure 2G-I)**.

Major Task 5: Regulatory approval of animal research experiments. An animal protocol describing the experiments envisioned under this proposal was approved by *Columbia University*'s *Institutional Animal Care and Use Committee* (IACUC) on 08/29/2019 **(Subtask 5.1)**. A matching protocol was submitted for review to the *Department of Defense* (DOD) *Animal Care and Use Office* (ACURO) on 12/13/2019, and approved by the DOD's ACURO on 03/17/2020 **(Subtask 5.2)**. During the 2nd and 3rd years of the award, the animal protocol was renewed (05/27/2021) and approved for continuation (05/25/2022) by *Columbia University*'s IACUC.

Major Task 6: Generation and validation of animal breast cancer models for the *in vivo* study of spontaneous metastasis. During the three years of the award, we engineered a variety of human and murine TNBC models to express both fluorescent (EGFP, ZsGreen) and bio-luminescent reporters (Luciferase), and then investigated the kinetics and tissue-tropism of their *in vivo* metastatic dissemination using non-invasive *bioluminescent imaging* (BLI) systems **(Subtasks 6.1-6.4)**.

Engineering of human and murine TNBC cell lines (4T1, MDA-MB-231, MDA-MB-468) with lentivirus constructs encoding for Luciferase reporter genes (Subtask 6.1). As a first step, we identified three (n=3) TNBC cell lines that could be used as appropriate experimental models for the *in vivo* arm of the study, based on their reported capacity to spontaneously metastasize in animals: **4T1** (mouse; ATCC #CRL-2539), **MDA-MB-231** (human; ATCC #HTB-26), **MDA-MB-468** (human; ATCC #HTB-132). We then infected all three cell lines with two distinct lentivirus vectors encoding for both fluorescent (EGFP, ZsGreen) and bio-luminescent reporters (Luciferase): 1) pLentiLox3.7-mcs-IRES-Luciferase/EGFP, which was generated in-house by modification of the pLentiLox3.7 backbone (Addgene #11795); and 2) and the **pHIV-Luc2P-ZsGreen** (Addgene #39196). Our experimental results led to two key observations: 1) shortly after infection with the pLentiLox3.7-mcs-IRES-Luciferase/EGFP vector, 4T1 cells, which are murine in origin, rapidly and permanently lost EGFP expression, while they retained expression of ZsGreen following infection with the pHIV-Luc-ZsGreen vector; this observation suggested that 4T1 cells, might be able to silence the *Cytomegalovirus* (CMV) promoter (which drives the expression of EGFP in the pLentiLox3.7 backbone), but not of the *Eukaryotic Translation Elongation Factor 1 Alpha* (EF1a) promoter (which drives the expression of ZsGreen in the pHIV-Luc-ZsGreen backbone), in a manner that is reminiscent to what observed in mouse *embryonic stem* (ES) cells (Meilinger *et al.*, *EMBO Reports*, 10:1259-64, 2009); 2) in human TNBC cell lines (MDA-MB-231, MDA-MB-468), the intensity of green fluorescent signals observed following infection with the pHIV-Luc-ZsGreen vector were higher than those observed following infection with the pLentiLox3.7-mcs-IRES-Luciferase/EGFP vector, even after exclusion of un-infected cells, indicating a superior performance of the pHIV-Luc-ZsGreen vector as a reporter for *in vitro* and *in vivo* assays. We, therefore, proceeded to use *fluorescence activated cell sorting* (FACS) for the isolation of infected cells (ZsGreen^{+}) from mixed cultures infected with the pHIV-Luc-ZsGreen construct, leading to the generation of sub-lines expressing the reporter genes at 99-100% purity and in a stable manner **(Figure 5)**.

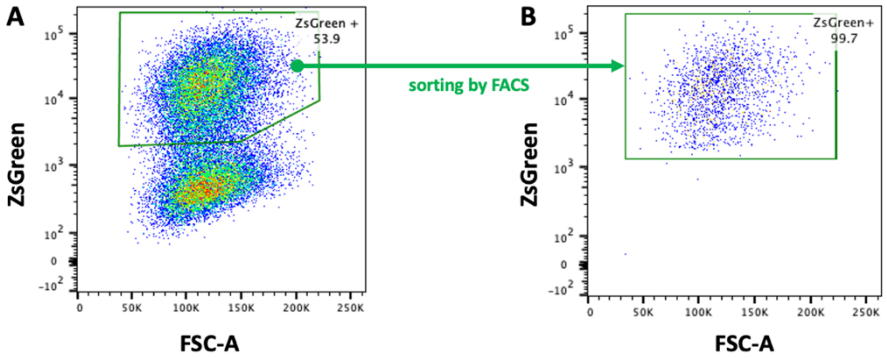

Figure 5. Generation of *triple-negative breast cancer* (TNBC) cell lines engineered to express fluorescent reporters. (A) Following infection with the pHIV-Luc-ZsGreen lentivirus vector, the MDA-MB-231 breast cancer cell line was analyzed by flow cytometry and observed to express high levels of green fluorescence in a substantial percentage (54%) of cells. **(B)** MDA-MB-231 cells expressing high levels of green fluorescence (ZsGreen^{+}; green gates) were sorted by *fluorescence activated cell sorting* (FACS), and propagated *in vitro* as pure sub-line (>99% ZsGreen^{+}).

Time-course studies on the kinetics and tissue tropism of spontaneous metastatic dissemination of human and murine TNBC cell lines (Subtask 6.2). As a second step, we tested whether all three TNBC cell lines that we engineered to express a bio-luminescent reporter (i.e. the Luc2P variant of the firefly Luciferase) could be *"tracked"* in terms of their anatomical location following *in vivo* injection in mice, based on the emission of bright and specific bio-luminescent signals that could measured using an *IVIS Spectrum* machine PerkinElmer **(Figure 6)**. Our results indicated that all three TNBC lines could form solid tumors at primary injections sites, and also display reproducible growth kinetics across biological replicates (i.e. equal doses of cells from the same cell line appear to undergo

numerical expansion with similar mathematical functions across different animals, when evaluated using quantitative measurements of their bio-luminescent signal).

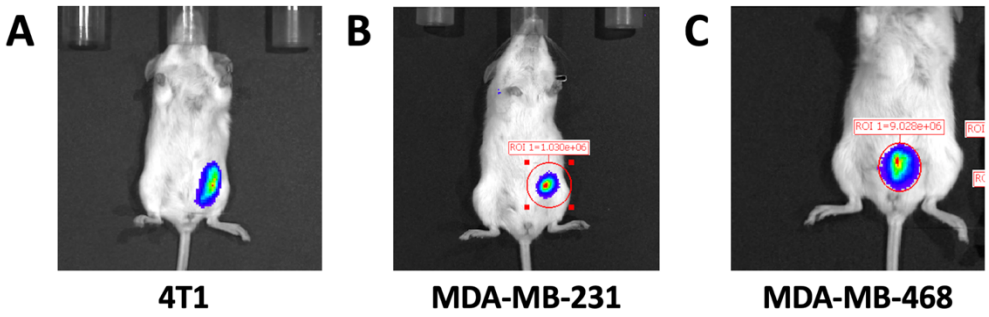

Figure 6. Detection of bio-luminescent signals from TNBC cell lines infected with the pHIV-Luc-ZsGreen lentivirus vector and injected *in vivo*, in the *sub-cutaneous* (s.c.) tissue of female mice. Following infection with the pHIV-Luc-ZsGreen lentivirus vector and purification by FACS, three TNBC cell lines were injected s.c. in female mice. In all three cases, the anatomical location of injected tumor cells could be readily detected based on the generation of a bio-luminescent signal following intra-peritoneal injection of luciferin (150 mg/kg). **(A)** 4T1 cells (murine) injected in Balb/c mice. **(B)** MDA-MB-231 cells (human) and **(C)** MDA-MB-468 cells (human), injected in NOD/SCID/IL2R$\gamma^{-/-}$ (NSG) mice.

During the first three years of the award (07/15/2019-07/14/2022), we conducted longitudinal time-course studies aimed at elucidating the kinetics of metastatic spread for the two cell lines that displayed the fastest growth rates (4T1, MDA-MB-231). Our results indicated that both human (MDA-MB-231) and murine (4T1) TNBC models were able to efficiently metastasize *in vivo* to the lungs, although with different kinetics **(Figure 7A)**. The 4T1 model (murine) appeared able to disseminate very rapidly (appearance of a measurable increase in bioluminescent signal from the thoracic region: days 7-14 after injection), while the MDA-MB-231 model (human) disseminated more slowly (appearance of a measurable increase in bioluminescent signal from the thoracic region: days 77-91 after injection). These observations provided important insights in the design of *in vivo* experiments. For example, our data indicated that, in the case of the 4T1 model, in order to correctly evaluate the capacity of NABNPs to prevent metastatic dissemination, our experimental design would need to envision treatment initiation immediately after the sub-cutaneous cell injection of the cancer cells. Otherwise, results might be inconclusive due to the metastatic lesions in the lungs being already established before treatment initiation. On the other hand, in the case of the MDA-MB-231 model, treatment would have to be initiated 7 weeks after injection (day 49), in order to allow for a full treatment cycle (7 weeks) to initiate before lung metastases are established (day 77), and be completed before control animals treated with saline solution would require to be euthanized (day 112), due to the progressive growth of sub-cutaneous primary tumors, which would reach maximum allowable diameters **(Figure 7B)**.

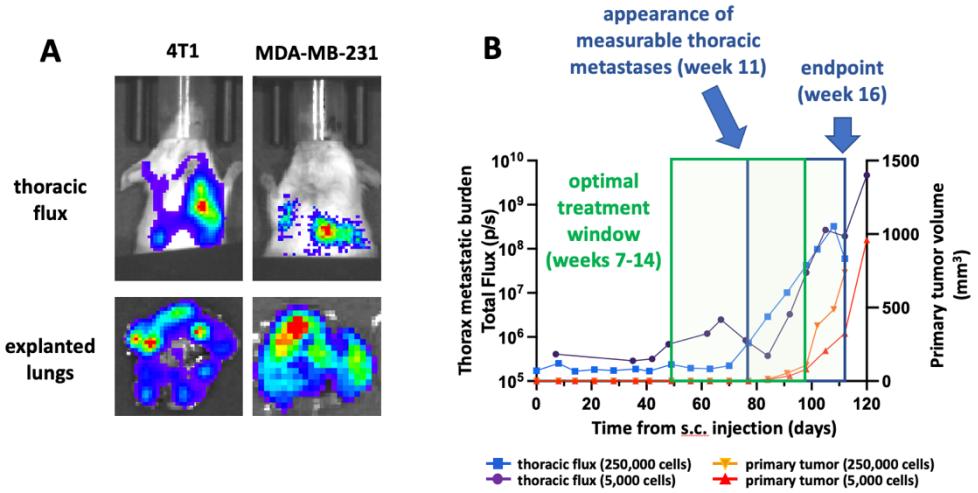

Figure 7. Non-invasive monitoring of the *in vivo* kinetics of metastatic spread of TNBC breast cancer cells. (A) Following s.c. injection in female mice, both 4T1 and MDA-MB-231 cells were able to spontaneously metastasize to the lungs, as revealed by the *bio-luminescent imaging* (BLI) of the animals' thoracic area and explanted lungs. **(B)** In the case of human MDA-MB-231 cells injected sub-cutaneously (s.c.) in NOD/SCID/IL2R$\gamma^{-/-}$ (NSG) mice, the kinetics of *in vivo* spread were relatively slow, with lung metastases becoming measurable by *ex vivo* imaging at 11 weeks after injection.

Engineering of human TNBC *patient-derived xenograft* (PDX) lines with lentivirus constructs encoding for Luciferase reporter genes (Subtask 6.3). Although 4T1 and MDA-MB-231 cell lines represent useful models for the study of breast cancer metastasis, they both display one important limitation: they are unable to accurately recapitulate the cellular complexity of human primary tumors, especially with regard to their heterogeneous repertoire of malignant cell phenotypes (e.g., cells of basal and ductal lineages, cells with stem cell phenotypes). In order to overcome this limitation, we decided to use *patient-derived xenograft* (PDX) models (i.e., tumors originated by direct implantation of human primary malignant tissues in immune-deficient mice), because they retain and recapitulate many of the key biological features of the original disease, not only with respect to its repertoire of somatic mutations, but also with regard to its histology (e.g., three-dimensional architecture, cellular composition) and drug sensitivity. We, therefore, proceeded to engineer with a bioluminescent reporter (Luc2P) three (n=3) *patient-derived xenograft* (PDX) lines identified as appropriate experimental models for the study: **TM-00089**, **TM-00096** and **TM-00098** (all three established from human TNBCs and commercially available from *The Jackson Laboratory*). The three PDX lines were engrafted sub-cutaneously in NOD/SCID/IL2R$\gamma^{-/-}$ (NSG) mice and allowed to form palpable tumors. Tumors were then harvested and dissociated, and human malignant cells purified by FACS, infected with the pHIV-Luc-ZsGreen lentivirus vector and re-injected in secondary hosts. *Bioluminescent imaging* (BLI) of secondary hosts revealed the presence of a strong signal in correspondence of tumors appearing at injection sites **(Figure 8)**, confirming successful engineering of all three PDX lines with Luc2P.

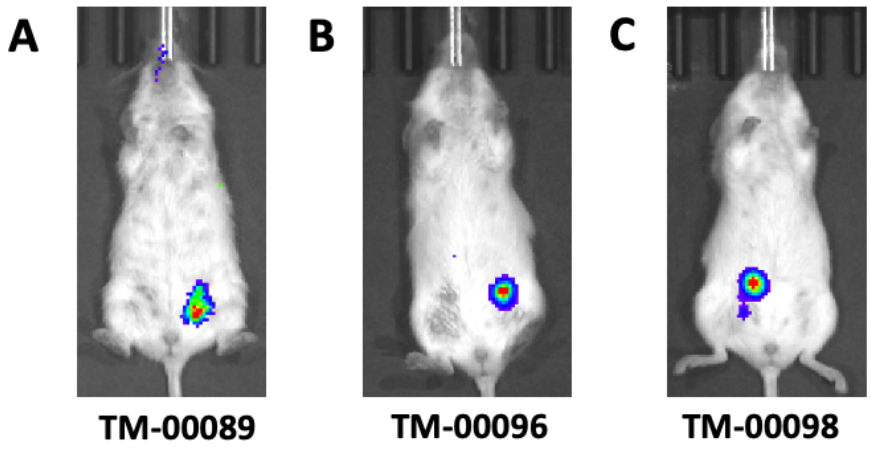

Figure 8. Detection of bio-luminescent signals from TNBC *patient-derived xenograft* (PDX) lines infected with the pHIV-Luc-ZsGreen lentivirus vector and injected *in vivo*, in the *sub-cutaneous* (s.c.) tissue of female mice. Following purification by FACS and infection with the pHIV-Luc-ZsGreen lentivirus vector, human malignant cells from three independent TNBC PDX lines (**A**: TM-00089; **B**: TM-00096; **C**: TM-00098) were injected s.c. in NOD/SCID/IL2R$\gamma^{-/-}$ (NSG) female mice. In all three cases, injected tumor cells could be readily detected in correspondence of injection sites, based on the appearance of a bio-luminescent signal, following luciferin administration (150 mg/kg, i.p.).

Evaluation of human PDX lines with regard to their capacity to metastasize *in vivo* (Subtask 6.4). In order to ensure both maximum accuracy and maximum sensitivity in the conduction of studies aimed at the quantification of spontaneous metastatic dissemination in immune-deficient mice, we decided to develop PDX lines in which the malignant component was uniformly labeled with fluorescent (ZsGreen) and bioluminescent (Luciferase) reporters **(Figure 9A)**. In the specific case of PDX models, this operation is relatively long and laborious, because PDX lines are propagated by serial grafting of solid tissues *in vivo* (as opposed to 4T1 and MDA-MB-231 models, which can be propagated as cell cultures *in vitro*). During the 3rd year of the award, however, we were able to leverage our long-standing expertise with *fluorescence-activated cell sorting* (FACS) in order to isolate, and then selectively transplant in immune-deficient hosts, the sub-set of human malignant cells that were engineered by lentivirus infection to express fluorescent reporters. We repeated this operation of selective enrichment over 2-3 rounds of serial passaging, eventually achieving 100% purity **(Figure 9B)**. Once the human component (EpCAM^{+}) of a PDX line was confirmed to consist exclusively of genetically engineered cells (ZsGreen^{+}), we proceeded to evaluate its capacity for spontaneous *in vivo* metastasis, once again by conducting longitudinal BLI studies. In the case of the **TM-00098** PDX line, s.c. injection of purified

malignant cells into NSG female mice was followed not only by rapid tumor growth at the primary injection site **(Figure 9C)**, but also by spontaneous metastasis to the lungs and liver **(Figure 9D-E)**.

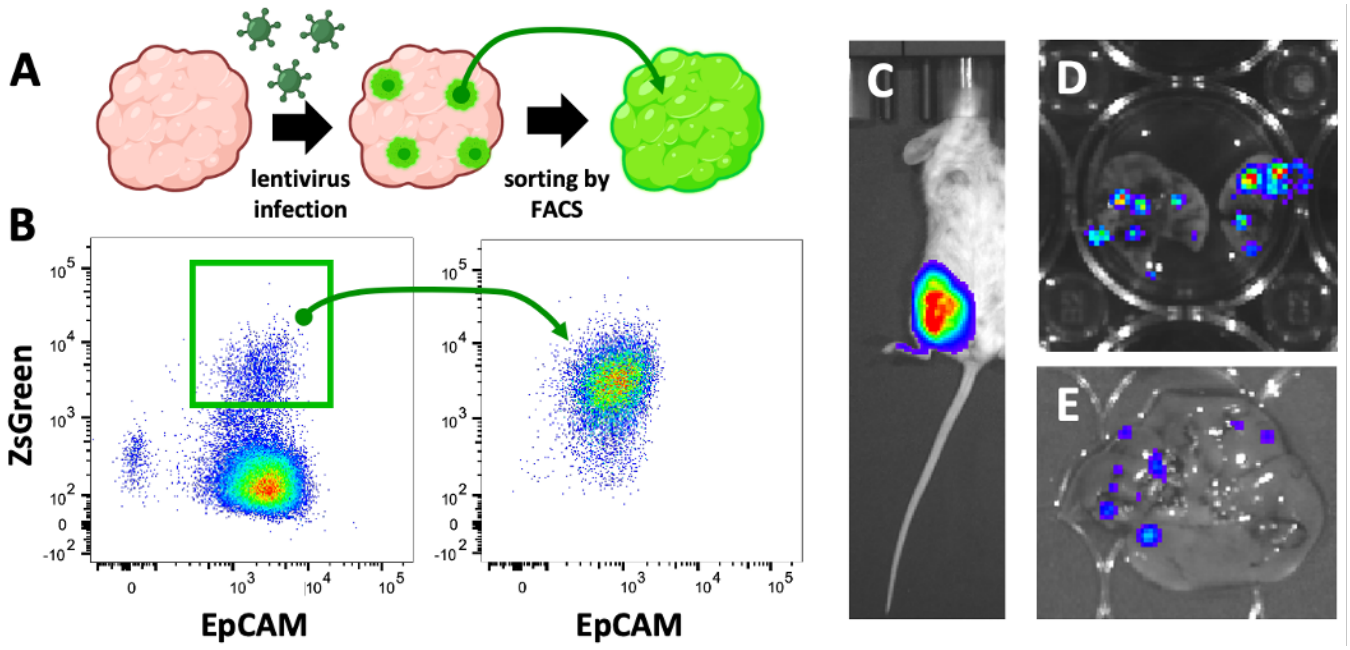

Figure 9. Genetic engineering of the TM-00098 *patient-derived xenograft* (PDX) line and demonstration of its spontaneous metastatic dissemination in living organisms. (A) Schematic representation of the experimental workflow implemented to produce TNBC PDX lines with uniform expression of fluorescent and bioluminescent reporters: malignant cells were infected with lentivirus vectors encoding for both a fluorescent (ZsGreen) and a bioluminescent (Luciferase) reporter, and then purified by *fluorescence-activated cell sorting* (FACS) based on the differential expression of the fluorescent reporter, to achieve 100% purity. **(B)** Scatter plots displaying expression of the fluorescent reporter (ZsGreen) in human malignant cells ($EpCAM^+$) from the TM-00098 PDX line, before and after purification of infected cells by FACS, confirm achievement of 100% purity. **(C)** Injection of genetically engineered TM-00098 cells in the s.c. tissue of NSG female mice was followed by rapid growth and emission of a robust bio-luminescent signal. **(D-E)** Animals engrafted with the TM-00098 PDX line developed multiple metastatic lesions in the lungs (D) and in the liver (E).

Major Task 7: Evaluation of the *in vivo* pharmacokinetics, bio-distribution and accumulation across tissues of PAMAM-G3-$C12_5$-$DEEA_{20}$ NABNPs (NP^+). During the three years of the award, our research teams completed a set of joint experiments that were aimed at studying the bio-distribution of PAMAM-G3-$C12_5$-$DEEA_{20}$ NABNPs (NP^+) in tumor-bearing animals, with a special focus on understanding whether they would preferentially accumulate in malignant as opposed to normal tissues, and whether NABNPs loaded with a chemotherapy agent of the taxane family (e.g., paclitaxel) would display a therapeutic activity against primary tumors that is comparable or superior to that of an equal dose of the same agent administered alone **(Subtasks 7.1-7.2).**

Evaluation of the therapeutic activity of PAMAM-G3-$C12_5$-$DEEA_{20}$ NABNPs (NP^+) against primary tumors. To evaluate the *in vivo* bio-distribution of PAMAM-G3-$C12_5$-$DEEA_{20}$ NABNPs (NP^+) and understand whether they would be able to deliver meaningful payloads of anti-tumor agents into primary tissues, we engrafted 4T1 cells in the sub-cutaneous tissue of Balb/c mice, and allowed them to develop palpable tumors. We then injected tumor-bearing animals with PAMAM-G3-$C12_5$-$DEEA_{20}$ NABNPs (NP^+), either alone or loaded with *paclitaxel* (PTX), and finally evaluated the activity of the PTX-loaded NABNPs against primary tumors as compared to that of sham injections (e.g., saline solution) and PTX administered alone **(Figure 10)**. The results showed that, while administration of *"empty"* PAMAM-G3-$C12_5$-$DEEA_{20}$ NABNPs (NP^+) had no direct anti-tumor activity against established s.c. lesions, administration of PAMAM-G3-$C12_5$-$DEEA_{20}$ NABNPs (NP^+) loaded with PTX was associated with a reduction in tumor growth kinetics and an extension of mouse survival, superior in magnitude to that observed when administering PTX alone or other NABNP formulations loaded with PTX **(Figure 10A-B)**. To understand whether the increased anti-tumor activity of PTX-loaded PAMAM-G3-$C12_5$-$DEEA_{20}$ NABNPs (NP^+) was due to enhanced cytotoxic effects on malignant cells, we analyzed tumor tissues harvested from treated animals for evidence of increased apoptosis and

reduced proliferation. Indeed, the results showed that tumors harvested from animals treated with PTX-loaded PAMAM-G3-C12$_5$-DEEA$_{20}$ NABNPs (NP$^+$) were characterized by higher percentages of apoptotic cells (TUNEL$^+$) and lower percentages of mitotic cells (Ki67$^+$) as compared to controls, such as tumors from control animals treated with saline solution, PTX alone or other NABNP formulations loaded with PTX **(Figure 10C-E)**.

Evaluation of the *in vivo* biodistribution of PAMAM-G3-C12$_5$-DEEA$_{20}$ NABNPs (NP$^+$) in tumor-bearing animals. To understand whether the increased anti-tumor activity displayed by PTX-loaded PAMAM-G3-C12$_5$-DEEA$_{20}$ NABNPs (NP$^+$) could be explained by the capacity of NABNPs to preferentially accumulate within tumor tissues (and thus deliver higher payloads of PTX to cancer cells), we labeled a variety of NABNP formulations with a fluorescent die (Cy5) and then injected them into tumor-bearing Balb/c mice engrafted with 4T1 cells. We then measured the intensity of the fluorescent signal in both tumor tissues and a variety of normal organs (e.g. heart, lungs, liver, spleen, kidneys) in order to compare the anatomical distribution of the different NABNP formulations **(Figure 10F-G)**. Our results revealed that, as compared to other NABNP formulations, PAMAM-G3-C12$_5$-DEEA$_{20}$ NABNPs (NP$^+$) tended to reach higher concentrations in tumor tissues, as well as in organs that are common sites of TNBC metastasis (e.g. lung, liver), and lower concentrations in other critical organs (e.g. heart, kidneys). These observations provided further evidence in support of the use of PAMAM-G3-C12$_5$-DEEA$_{20}$ NABNPs (NP$^+$) as *"carriers"* of therapeutic agents for the treatment of TNBCs, given their *in vivo* bio-distribution profile, which appears to privilege tumor tissues and organs frequently targeted by metastatic spread (e.g. lung, liver), while sparing functionally sensitive organs (e.g. heart, kidneys).

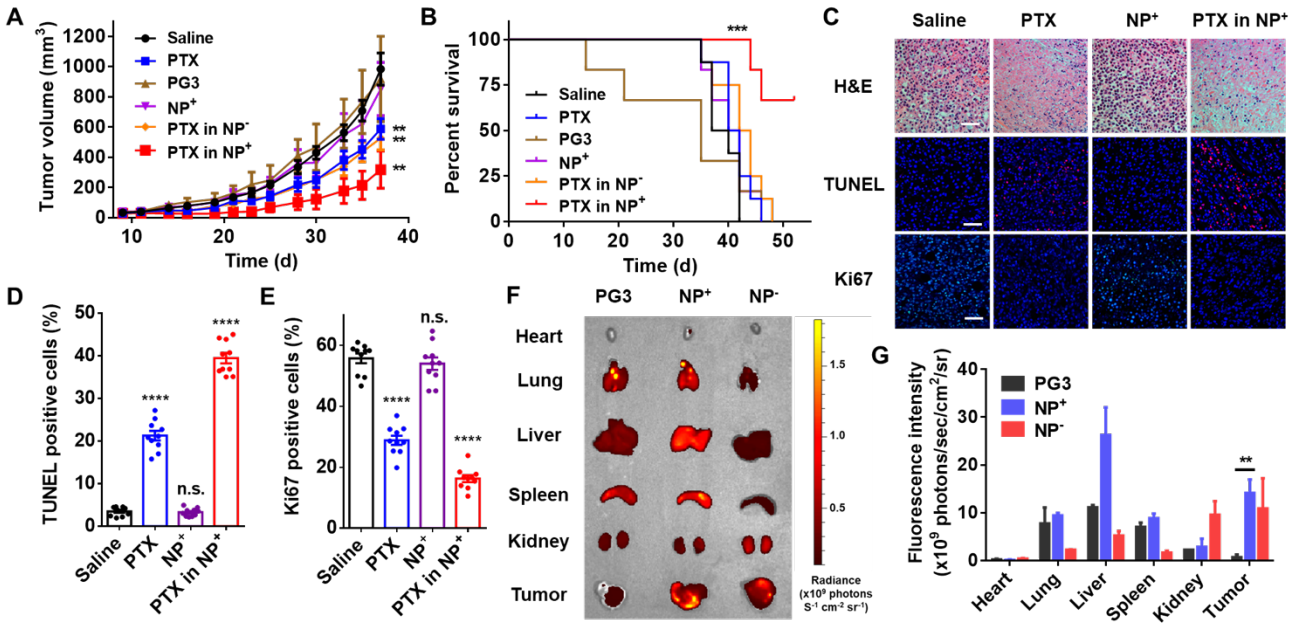

Figure 10. *In vivo* anti-tumor activity and bio-distribution of PTX-loaded PAMAM-G3-C12$_5$-DEEA$_{20}$ NABNPs (NP$^+$). **(A)** Growth kinetics of sub-cutaneous (s.c.) primary tumors in Balb/c mice engrafted with 4T1 breast cancer cells and treated with a variety of NABNP formulations (15 mg/kg, i.p.) either in the presence or absence of PTX (4.5 mg/kg., i.p.). Mice were sacrificed when s.c. tumor volumes exceeded 1000 mm^3. **(B)** Kaplan-Meier survival curves of treated animals. **(C)** Primary tumor tissues were stained with *hematoxylin and eosin* (H&E) and analyzed for the presence of apoptotic cells (TUNEL$^+$) and proliferating cells (Ki67$^+$). Scale bar: 50 µm. **(D-E)** Quantification of TUNEL$^+$ (D) and Ki67$^+$ (E) cells in primary tumors. **(F)** *Ex vivo* fluorescent imaging of organs explanted from mice injected with Cy5-labeled NABNPs (24 hours after i.p. injection). **(G)** Quantification of fluorescence intensity in different organs following injection with Cy5-labeled NABNPs. Data were compared with those from control animals receiving injections of saline solution, unless indicated otherwise. Statistical significance was calculated using Student's t test: *P<0.05, **P<0.01, ***P<0.001, ****P<0.0001. Error bars: mean ± SEM.

Major Task 8: Evaluation of the *in vivo* therapeutic efficacy of taxane-loaded PAMAM-G3-C12$_5$-DEEA$_{20}$ NABNPs (NP$^+$) in the 4T1 model of spontaneous metastasis. During the three years of the award, our research teams completed a set of joint experiments that were aimed at testing whether treatment of tumor-bearing animals with PAMAM-G3-C12$_5$-DEEA$_{20}$ NABNPs (NP$^+$) is able to scavenge the *circulating free* DNA (cfDNA) that progressively accumulates in the bloodstream of tumor-bearing

animals, thus reducing systemic inflammation and limiting the metastatic spread of cancer cells **(Subtasks 8.1-8.2)**.

Evaluation of PAMAM-G3-C12$_5$-DEEA$_{20}$ NABNPs (NP$^+$) as *in vivo* scavengers of cfDNA and anti-inflammatory agents in tumor-bearing animals. To understand whether PAMAM-G3-C12$_5$-DEEA$_{20}$ NABNPs (NP$^+$) would be able to bind and sequester (i.e. to *"scavenge"*) cfDNA in tumor bearing animals, we measured the levels of cfDNA in Balb/c mice engrafted with 4T1 cells, either in the presence or absence of treatment with various formulations of NABNPs **(Figure 11A-B)**. Our results revealed that, while in healthy animals (i.e., animals not engrafted with cancer cells) the levels of cfDNA remained unmodified over time, in tumor-bearing animals the levels of cfDNA increased dramatically, presumably as a result of the progressive increase in tumor burden. Most importantly, our results also showed that, while treatment with PTX alone tended to associate with an increase of cfDNA levels (presumably as a result of the killing of a fraction of the malignant cell population), treatment with PAMAM-G3-C12$_5$-DEEA$_{20}$ NABNPs (NP$^+$) was able to maintain cfDNA levels at baseline values, in essence preventing any tumor-associated increase in cfDNA, even when using PTX-loaded formulations. Importantly, treatment with PAMAM-G3-C12$_5$-DEEA$_{20}$ NABNPs (NP$^+$) was also able to prevent tumor-associated increases in the circulating levels of various pro-inflammatory cytokines (IL6, IL1β, TNFα), which are often associated with high levels of cfDNA **(Figure 11C-F)**.

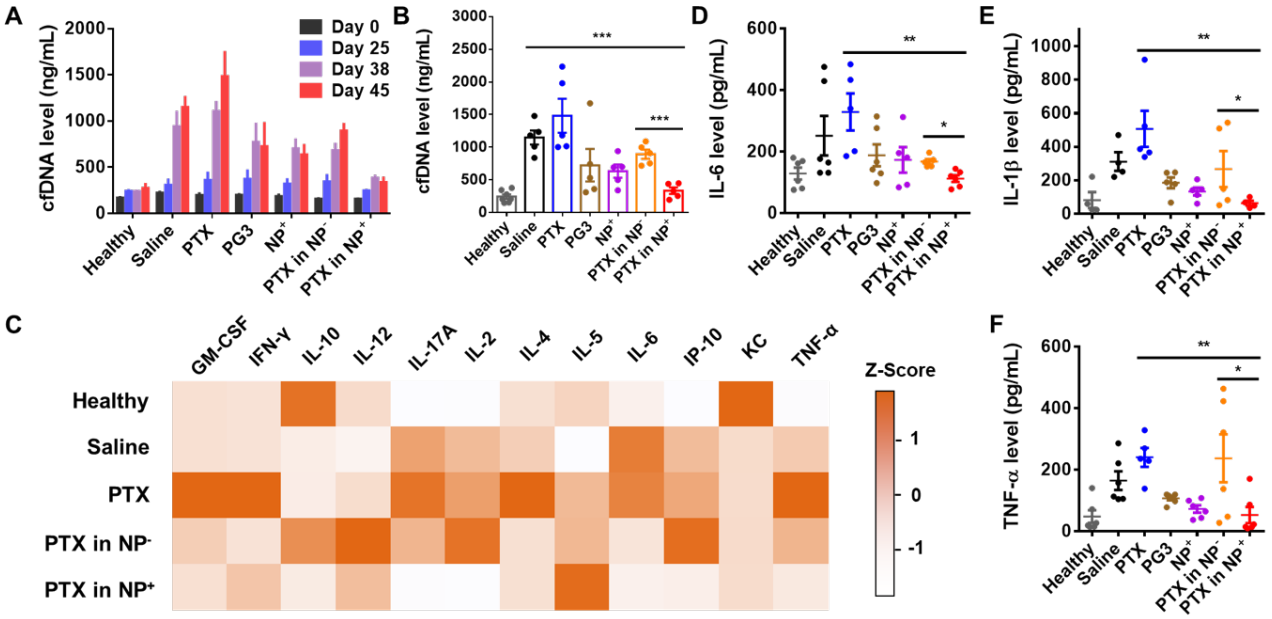

Figure 11. *In vivo* activity of PAMAM-G3-C12$_5$-DEEA$_{20}$ NABNPs (NP$^+$) as cfDNA scavengers and anti-inflammatory agents. (A-B) Measurement of cfDNA levels in the serum of tumor-bearing mice treated with various NABNP formulations. **(C)** Measurement of the serum levels of a panel of inflammatory cytokines (platform: IsoPlexis) in tumor-bearing mice treated with various NABNP formulations (only detectable cytokines are shown and cytokine levels are normalized to Z scores). **(D-F)** Measurement of the serum levels of IL-6 (D), IL-1β (E), and TNFα (F) in tumor-bearing mice treated with various NABNP formulations. All data are compared to those from healthy mice. Statistical significance is calculated using Student's t test. *P<0.05, **P<0.01, ***P<0.001 and ****P<0.0001. Error bars: mean ± SEM.

Evaluation of PAMAM-G3-C12$_5$-DEEA$_{20}$ NABNPs (NP$^+$) as therapeutic agents able to suppress the *in vivo* metastatic spread of breast cancer cells. To understand whether treatment with PAMAM-G3-C12$_5$-DEEA$_{20}$ NABNPs (NP$^+$) would be able to prevent the metastatic dissemination of breast cancer cells, we engrafted Balb/c mice with 4T1 cells engineered to constitutively express a bio-luminescent reporter (Luc2P), and then monitored them over time for the development of lung metastases, either in the presence or absence of treatment with PTX, as well as a variety of NABNP formulations, either in native form or pre-loaded with PTX **(Figure 12)**. Our results revealed that, while control animals (i.e., animals treated with saline solution) promptly developed a high burden of lung metastases, animals treated with PAMAM-G3-C12$_5$-DEEA$_{20}$ NABNPs (NP$^+$) did not, irrespective of the fact that NABNPs had been pre-loaded or not with PTX. Interestingly, our results also showed that treatment with PTX alone, although capable of limiting the growth of established tumors at the primary site, was nonetheless unable to prevent metastatic spread, and perhaps actively contributed to

exacerbate it (most likely by causing systemic inflammation, secondary to an increased release of cfDNA in the bloodstream of tumor-bearing animals, due to active cell killing at the tumor's primary site). Most importantly, our data showed that the drug formulation displaying the highest therapeutic activity (i.e. the highest degree of suppression of metastatic spread) was the PAMAM-G3-$C12_5$-$DEEA_{20}$ NABNPs (NP^+) formulation pre-loaded with PTX. This observation confirmed the scientific hypothesis at the foundation of our study: that the therapeutic activity of cytotoxic chemotherapy can be substantially enhanced by simultaneous administration of pharmacological agents that are able to *"scavenge"* the cfDNA that is released in the blood circulation as a result of the killing of tumor cells (because such cfDNA scavenging agents *"dampen"* the pro-inflammatory effects of cfDNA, and thus limit the capacity of surviving tumor cells to successfully metastasize, a process facilitated by the systemic inflammation mediated by TLR activation).

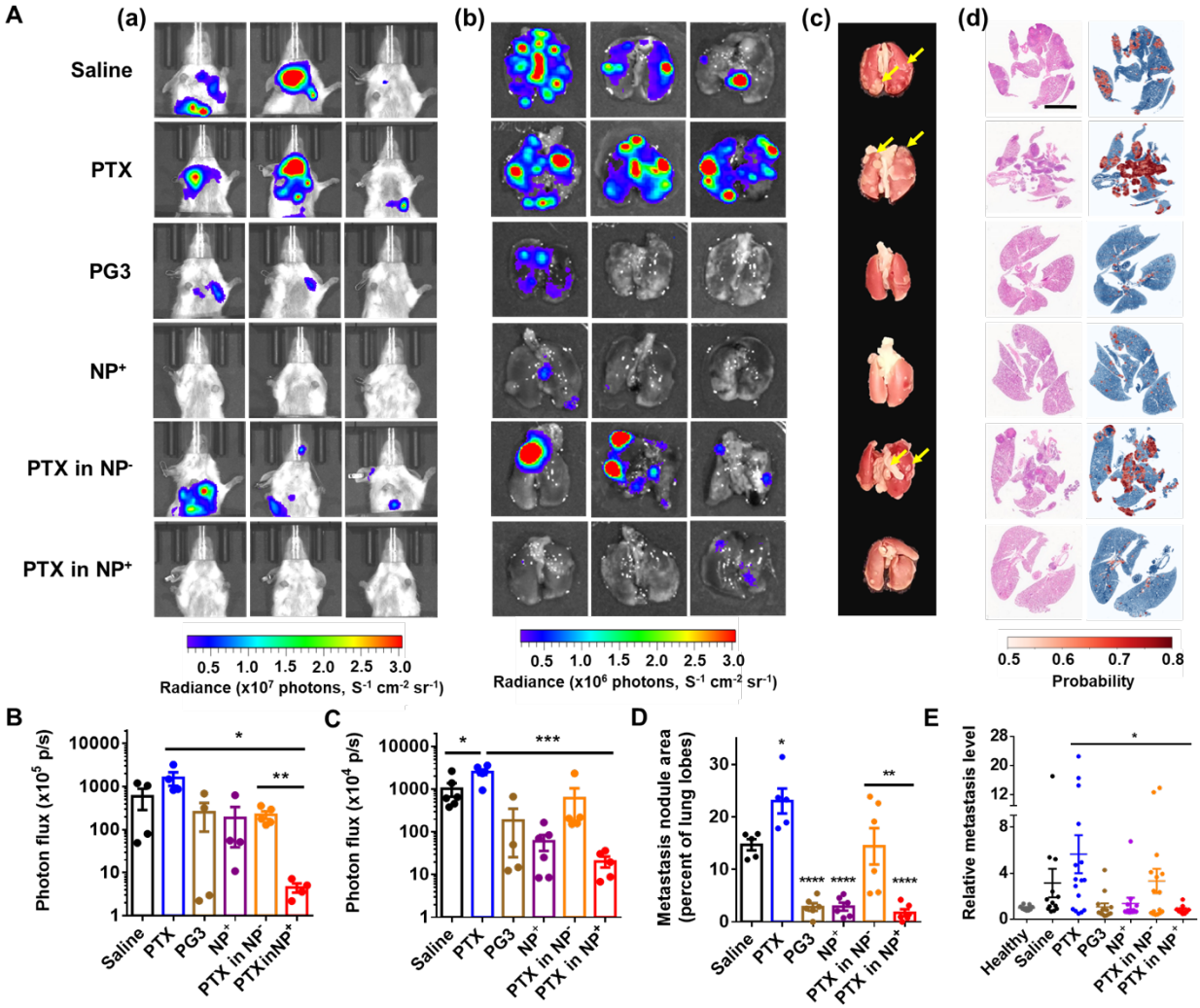

Figure 12 *In vivo* activity PTX-loaded PAMAM-G3-$C12_5$-$DEEA_{20}$ NABNPs (NP^+) as inhibitors of tumor metastasis. (A; a) Non-invasive imaging of bio-luminescent signals from the thoracic region of Balb/c mice injected s.c. with 4T1 cells, revealing metastatic spread to the lungs. **(A, b)** *Ex vivo* bio-luminescent imaging of explanted lungs (6 weeks after treatment initiation) confirming presence of live metastases. **(A, c)** Photograph of explanted lungs, confirming presence of metastatic nodules. **(A, d)** Computer-assisted analysis of tissue sections from metastatic lungs stained with H&E, generating probability maps for metastatic tissues (probability of metastatic identity for individual cells). Scale bar: 2 mm. **(B)** Quantification of photon flux from *in vivo bioluminescent imaging* (BLI). **(C)** Quantification of photon flux from *ex vivo* bioluminescent imaging. **(D)** Quantification of lung surface area consisting of metastatic nodules (percent). **(E)** Computer-assisted quantification of metastatic cells in lung sections (relative metastasis level: sum of probabilities across all cells). *P<0.05, **P<0.01, ***P<0.001, and ****P<0.0001 (Student's t-test). Error bars: mean ± SEM.

Major Task 9: Evaluation of the therapeutic efficacy of taxane-loaded NABNPs against human models of *triple-negative breast cancer* (TNBC). After having observed that PAMAM-G3-$C12_5$-$DEEA_{20}$ NABNPs can be successfully used to improve the therapeutic outcomes of chemotherapy in a murine model of TNBC (4T1), our team proceeded to validate the possibility of implementing a similar

type of cationic NABNPs also against human models of TNBC. During the third year of the award, we completed an additional set of joint experiments, aimed at testing whether treatment with taxane-loaded cationic NABNPs is able to improve therapeutic outcomes in animals engrafted with human TNBC cells, by scavenging cfDNA **(Subtask 9.1)** and limiting the metastatic spread of cancer cells **(Subtask 9.2)**.

Evaluation of the therapeutic activity of PTX-loaded PAMAM-G3-Cholesterol NABNPs against MDA-MB-231 cells. As a first step, we tested the therapeutic activity of cationic NABNPs against MDA-MB-231 cells, a human model of TNBC. As compared to mouse 4T1 cells, human MDA-MB-231 cells require engraftment in immune-deficient hosts (NSG mice) and display slower kinetics of metastatic spread **(Figure 7).** MDA-MB-231 cells, however, better reflect some of the key biological properties of the human disease (e.g., genetic background of malignant cells, repertoire of somatic mutations, drug sensitivity). In this specific experiment, we decided to use a novel chemical formulation of cationic NABNPs: PAMAM-G3-Cholesterol$_5$. Although PAMAM-G3-C12$_5$-DEEA$_{20}$ NABNPs represented a very promising nanocarrier formulation, their synthetic route was extremely laborious, hindering their viability as actionable candidates for clinical translation. We decided, therefore, to improve upon the backbone of PAMAM-G3 NABNPs and identified PAMAM-G3-Cholesterol$_5$ as an excellent alternative, because it was comparable to PAMAM-G3-C12$_5$-DEEA$_{20}$ in terms of both its cfDNA scavenging ability and cellular cytotoxicity (IC_{50}~200 μg/mL), but was much simpler to synthetize. With as few as two cholesterol residues, G3-Cholesterol becomes amphiphilic and self-assembles into a micellar structure that efficiently encapsulates lipophilic drugs (e.g., PTX, doxorubicin). G3-Cholesterol is similar in size to G3 (3.6 nm), and is expected to be readily excreted from the renal system. Because the number of cholesterol molecules conjugated to the PAMAM-G3 backbone can be controlled for up to 14 residues, we anticipate that PAMAM-G3-Cholesterol NABNPs will represent a flexible platform, and will enable us to fine-tune the release kinetics of encapsulated chemo-drugs. In this set of experiments, MDA-MB-231 cells were engineered to constitutively express a firefly luciferase **(Figure 6)** and were engrafted s.c. in female NSG mice. Tumor-bearing mice were treated according to a regimen designed based on our previous data on the kinetics of spontaneous MDA-MB-231 metastasis in mice **(Figure 7),** and were monitored for metastatic burden by non-invasive BLI **(Figure 13A)**. Tumor-bearing mice were treated with various chemotherapy formulations, including saline solution (negative control), paclitaxel (PTX), NABNPs (NPs), and PTX-loaded NPs. We used PAMAM-G3-Cholesterol$_5$ NABNPs with a size (125.0 ± 10.5 nm) and zeta potential (56.4 ± 1.1 mV) similar to those of PAMAM-G3-C12$_5$-DEEA$_{20}$ NABNPs **(Figure 13B)**. As observed against 4T1 cells, treatment with PTX-loaded NPs displayed superior activity against primary tumor growth, as compared to PTX alone **(Figure 13C-D)**.

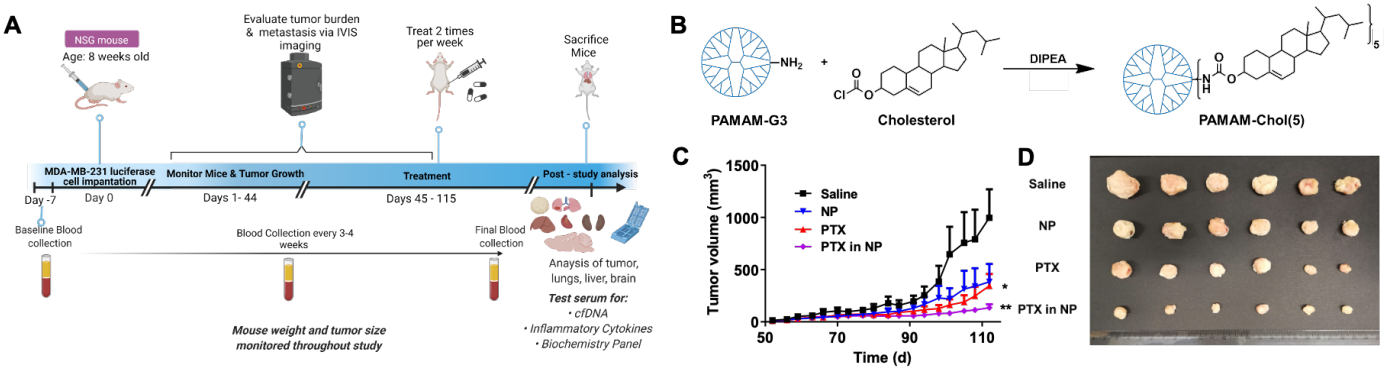

Figure 13. *In vivo* therapeutic activity of PTX-loaded NABNPs against a human TNBC model. (A) Schematic outline of the experiment used to test the therapeutic activity of PTX-loaded NABNPs against human MDA-MB-231 cells (created with BioRender.com). **(B)** Chemical structure of PAMAM-G3-Cholesterol$_5$. **(C-D)** Growth curves and photographs of primary tumors established by injection of MDA-MB-231 human TNBC cells in the s.c. tissue of NSG mice and treated with different therapeutic agents. NABNPs (15 mg/kg) and PTX (4.5 mg/kg) were administered via i.p. injection, two times a week. Mice were sacrificed after tumor volumes exceeded 1,000 mm^3. Error bars: mean ± SEM.

The spontaneous development of lung metastases was monitored by *bioluminescent imaging* (BLI), as MDA-MB-231 cells were engineered to constitutively express luciferase (Luc2P). In agreement with data previously collected using the 4T1 model, both *in vivo* longitudinal imaging **(Figure 14E-F)** and *ex vivo* imaging on harvested organs **(Figure 14G-H)** showed that treatment with NABNPs, either alone

or loaded with PTX, was associated with a substantial reduction in metastatic burden to the lungs as compared to treatment with saline or PTX alone. This observation was also confirmed by a computer-assisted histological analysis of lung tissues **(Figure 14I)**, which revealed a reduction in the area of lung tissue consisting of metastatic cells **(Figure 14J)**. Finally, treatment with NABNPs, either alone or loaded with PTX, was associated with a substantial reduction in cfDNA **(Figure 14K-L)**. Taken together, these observations further confirmed our research hypothesis, demonstrating that cationic NABNPs can enhance the therapeutic activity of conventional chemotherapy also in a human TNBC model.

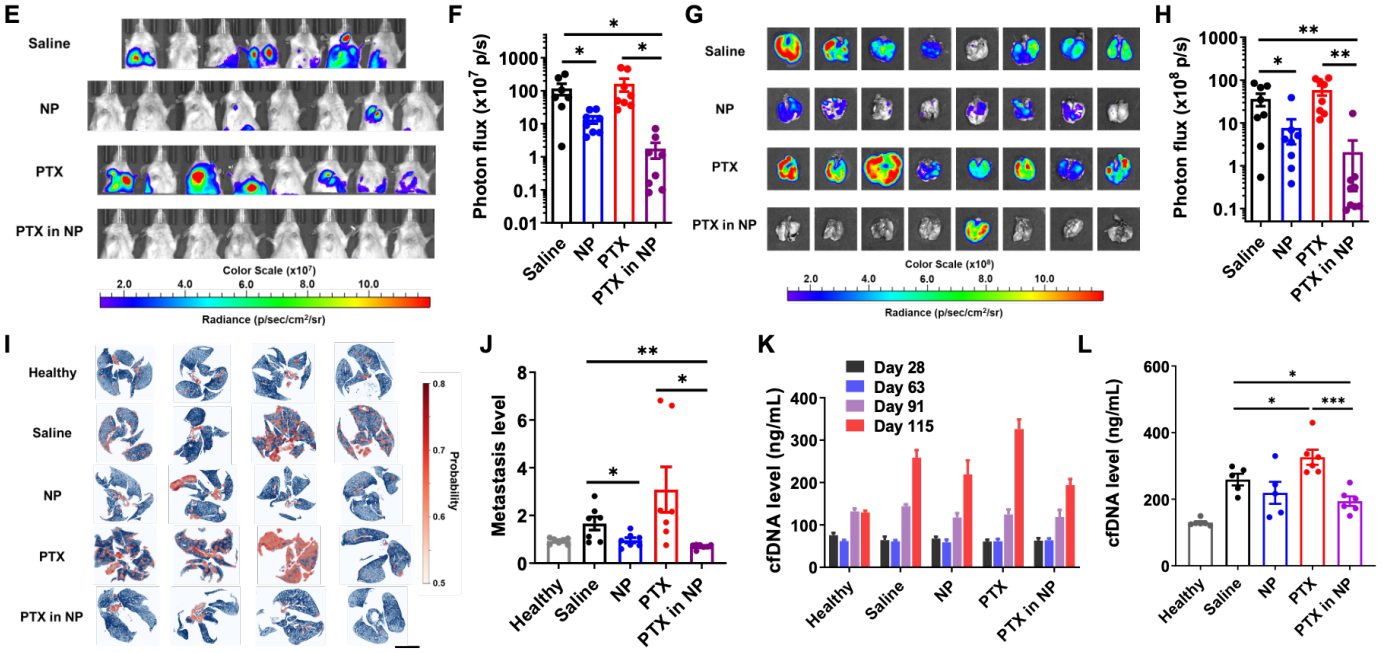

Figure 14. ***In vivo*** **therapeutic activity of PTX-loaded NABNPs against the MDA-MB-231 human TNBC model. (E)** *Bioluminescent imaging* (BLI) of the thoracic area of tumor-bearing mice on day 114 post-engraftment. Primary tumors were covered with black paper to shield their BLI signals, and enable detection of distant-site metastases. **(F)** Total photon flux from thoracic areas of tumor-bearing mice on day 114 post-engraftment. **(G)** *Ex vivo* BLI of isolated lungs immediately after euthanasia. **(H)** Total photon flux from isolated lungs. **(I)** Probability heat-maps generated by a computer-assisted machine-learning algorithm trained to identify metastatic cells. The probability heat-map indicates the probability for individual cells to represent metastatic cancer cells. Scale bar: 6 mm. **(J)** Quantification of the metastatic burden in lung sections, as estimated using the machine-learning algorithm. Metastatic burden was normalized to that of healthy animals. **(K)** Time-course evolution of cfDNA levels in the serum of NSG mice engrafted with MDA-MB-231 cells. **(L)** Comparison of cfDNA levels in the serum of NSG mice engrafted with MDA-MB-231 cells and treated with different chemotherapy formulations, as measured at the end of the experiment (day 115 post-engraftment), immediately before mice were sacrificed. *P<0.05, **P<0.01, ***P<0.001, ****P<0.0001 (Student's t test). Error bars: mean ± SEM.

Major Task 10: Preparation of a manuscript reporting on the study's results. A manuscript reporting on the first batch of experimental results obtained with the support of this award, including the data on the therapeutic activity of NABNPs as suppressors of spontaneous metastasis in both the 4T1 and MDA-MB-231 models, was recently accepted for publication:

Li T., Akinade T., Zhou J., Wang H., Tong Q., He S., Rinebold E., Valencia Salazar L.E., Bhansali D., Zhong Y., Ruan J., Du J., Dalerba P., and Leong K.W. *Therapeutic nanocarriers inhibit chemotherapy-induced breast cancer metastasis.* **Advanced Science**, e2203949, e-pub October 11, 2022.

PMID 36220339: https://pubmed.ncbi.nlm.nih.gov/36220339

Opportunities for training and professional development. During the 3rd year of the award (07/15/2021-07/14/2022), the trainees who participated in the research supported by this award were:

1) **Tianyu Li, PhD** (postdoctoral fellow, training in biomaterials and drug delivery)
2) **Tolu Olatokunbo Akinade, PhD** (MD/PhD student in Department of Biomedical Engineering)
3) **Siyu He, BS** (PhD student in Department of Biomedical Engineering)

4) **Ozgenur Celik, BS** (Master degree student in Department of Biomedical Engineering)

At the core of training activities for all trainees, including graduate students and post-doctoral fellows, is the preparation of an ***Individual Development Plan*** **(IDP),** which is used to help trainees learn how to actively manage the development of their professional career. IDPs are initially developed by the trainees, and subsequently discussed with their primary mentors, on a periodic basis. To provide guidance in the preparation of IDPs, all trainees, including graduate students and post-doctoral fellows, are offered the opportunity to enroll in *Columbia University*'s institutional IDP program, which is designed to help them develop strategies to actively manage their professional career, including the preparation of carefully structured IDPs. Program participants are engaged in coursework designed to help them become familiar with a variety of career options, and understand which skills (and professional experiences) are considered necessary to successfully pursue each career path. As part of their involvement in the educational activities included in the IDP program, participants acquire skills that are relevant to multiple career paths (e.g. how to write a research proposal, how to prepare for a job-talk). More specifically, graduate students and post-doctoral fellows enrolled in the IDP program learn how to: 1) identify career options; 2) devise strategies to actively manage career trajectories; 3) devise an IDP using the "myIDP" or "ImaginePhD" online tools; 4) utilize their IDP to share short-term and long-term career development plans with their mentors; 5) acquire skills that are considered critical to the successful pursuit of a variety of career paths (e.g. effective writing and oral communication skills); and 6) participate in professional networking events, designed to enable them to become familiar with the full spectrum of career opportunities that are most suited to their scholarly and scientific expertise. A comprehensive description of Columbia University's IDP program can be found at: https://research.columbia.edu/idp-program-2019-2020

In the laboratory setting, the trainees had the opportunity to interact with their PI on a weekly (if not daily) basis, discussing the progress of their experiments, as well as means to address emerging problems, in order to ensure that the research project proceeds on schedule. Within the PI laboratory, all trainees attended periodic laboratory meetings, during which they presented the results of their experiments, discussed their interpretation with mentors and peers, and received guidance on how to chart their path forward based on intellectual feed-back from all members of the research team.

In terms of technical skills, the trainees had the opportunity to become proficient in a variety of experimental techniques with which they were not previously familiar, such as: 1) the use *fluorescence activated cell sorting* (FACS) to achieve the selective purification of cancer cells engineered to express fluorescent reporters, which is critical when working with human *patient-derived xenograft* (PDX) lines that are propagated *in vivo* and cannot be easily sub-cloned using conventional *in vitro* tissue-culture techniques; 2) the use of non-invasive imaging platforms for the quantification of bio-luminescent signals from living animals (*IVIS Spectrum*; PerkinElmer), which can be applied to visualize the anatomical location of cancer cells engineered to express bio-luminescent reporters (Luciferase), and thus investigate the kinetics and tissue-tropism of their *in vivo* metastatic dissemination; 3) the use of automated platforms for high-throughput digital microscopy (*Cytation-5*; BioTek), which enable time-lapse studies of *in vitro* cell growth, and the computer-assisted quantification of perturbations in their proliferation kinetics; and 4) the application of computer-assisted, deep-learning techniques to analyze the histological samples and obtain quantitative comparisons for the extent of metastatic burden in an unbiased and rigorous manner.

Dissemination of results to communities of interest. Some of the results obtained in this study were presented at the following conferences, workshops and/or symposia:

1) "*Design of biomaterials to modulate inflammation"*, ***Joint Symposium of the Society for Biomaterials and the Japanese Society for Biomaterials***, Honolulu (Hawaii), January 8-10 (2022),

2) "*Design of biomaterials to modulate inflammation"*, ***Tissue Talks*** **of the** ***Department of Biomedical Engineering***, Columbia University, New York (New York), February 23 (2022)

3) "*Design of biomaterials for inflammatory diseases*", ***Seminars of the Department of Biomedical Engineering***, Yale University, New Haven (Connecticut), March (2022)

4) "*Design of biomaterials for inflammatory diseases*", ***Spring Meeting of the Korean Society of Biotechnology and Bioengineering*** **(KSBB)**, Daejeon (South Korea), April 13-15 (2022)

Research plans for the no-cost extension period. Over the next reporting period (07/15/2022-07/14/2023), which corresponds to a *no-cost extension* (NCE) period for this award, we aim to complete a major task that remained unaddressed **(Major Task 3)** and also propose to test whether PAMAM-G3-Cholestrol NABNPs can be leveraged to mitigate chemotherapy-induced cognitive impairment ("chemo-brain"). Chemotherapy-induced cognitive impairment is a debilitating side effect afflicting over two-thirds of cancer patients undergoing chemotherapy **[1-2]**. Breast cancer survivors consistently report experiencing problems with concentration, working memory and multi-tasking, pointing to changes in executive function and learning/memory **[1]**. *"Chemobrain"* can persist for 4-10 years after treatment, with subjects displaying hypo-responsiveness in the para-hippocampal gyrus during paired associate task assessments for episodic memory **[3]**. Oxidative stress, inflammation and telomere shortening have been implicated as contributing factors to chemobrain **[4]**. Chemotherapy induces a state of chronic inflammation, associated with increased levels of inflammatory cytokines in both the circulation and central nervous system **[5]**. Neuro-inflammation is a known risk factor in the patho-physiology of depression, which associates with chemobrain. As such, it is hypothesized that inflammation is linked with the pathophysiology of chemobrain. Encouraged by our results that PG3-Chol can reduce the levels of inflammatory cytokines in systemic circulation during chemotherapy, we would like to broaden the study to evaluate its effects on neuroinflammation and, consequently, chemobrain. In this set of experiments, we will switch to doxorubicin (DOX), for the following reasons:

1) DOX is a well-established cause of *"chemobrain"*. The underlying mechanism is presumed to be cytokine-induced oxidative stress and nitrosative damage to the CA1 hippocampal region **[6]**. Rats treated with DOX for 4 weeks display increased levels of pro-inflammatory cytokines (IL-6, IL-8, CXCL1) in both the systemic circulation and the brain **[2]**. Additionally, DOX-treated mice display increased TNFα levels in the hippocampus, which associate with memory impairment **[7]**;

2) DOX is a "cornerstone" of chemotherapy against breast cancer, in combination with other cytotoxic agents (e.g., in the AC-T regimen, consisting of doxorubicin, cyclophosphamide and paclitaxel);

3) It would be important to confirm that our idea of using NABNPs to increase drug-delivery to tumor sites while simultaneously scavenging cfDNA, thus obtaining a double "push-pull" therapeutic effect (i.e., *"pushing"* cytotoxing agents to tumor tissue, while simultaneously *"pulling"* cfDNA from the circulation) is applicable to more than one chemotherapy drug (i.e., it can be generalized).

References

1. Park H-S., Kim C-J., Kwak H-B., No M-H., Heo J-W. and Kim T-W. *Physical exercise prevents cognitive impairment by enhancing hippocampal neuroplasticity and mitochondrial function in doxorubicin-induced chemobrain.* **Neuropharmacology**, 133:451-461 (2018).
2. Vieira Cardoso C., Paes de Barros M., Lacerda Bachi A.L., Bernardi M.M., Berthi Kirsten T., de Fátima Monteiro Martins M., Dell'Armelina Rocha P.R., da Silva Rodrigues P. and Fernandes Bondan E. *Chemobrain in rats: behavioral, morphological, oxidative and inflammatory effects of doxorubicin administration.* **Behavioural Brain Research**, 378:112233 (2020).
3. Fardell J.E., Vardy J., Johnston I.N., and Winocur G., *Chemotherapy and cognitive impairment: treatment options.* **Clinical Pharmacology & Therapeutics**, 90:366-376 (2011).
4. Werfel T.A., Elion D.L., Rahman B., Hicks D.J., Sanchez V., Gonzales-Ericsson P.I., Nixon M.J., James J.L., Balko J.M., Scherle P.A., Koblish H.K. and Cook R.S. *Treatment-induced tumor cell apoptosis and secondary necrosis drive tumor progression in the residual tumor microenvironment through MerTK and IDO1.* **Cancer Research**, 79:171-182 (2019).
5. Salmena L, Poliseno L, Tay Y, Kats L, and Pandolfi PP, *A ceRNA hypothesis: the Rosetta Stone of a hidden RNA language?* **Cell**, 146:353-358 (2011).
6. El-Agamy S.E., Abdel-Aziz A.K., Wahdan S., Esmat A. and Azab S.S., *Astaxanthin ameliorates doxorubicin-Induced cognitive impairment (chemobrain) in experimental rat model: impact on oxidative, inflammatory and apoptotic machineries.* **Molecular Neurobiology**, 55:5727-5740 (2018).

7. Wang X-M., Walitt B., Saligan L., Tiwari A.F.Y., Cheung C.W., and Zhang Z-J, *Chemobrain: a critical review and causal hypothesis of link between cytokines and epigenetic reprogramming associated with chemotherapy.* **Cytokine**, 72:86-96 (2015).

4. IMPACT

Impact on the principal discipline of the project. The results of the experiments performed with the support of this award have contributed to important advances in two areas of **breast cancer** biology:

1) **Identification of NABNP formulations that can be successfully used as *in vivo* scavenging agents for cfDNA, and formal demonstration of their therapeutic activity as suppressors of metastatic dissemination in breast cancer.** The most important advancement made as a result of this study consists in the formal demonstration of the two core elements of the scientific hypothesis that underpinned it: 1) that cationic PAMAM dendrimers can be chemically engineered in order to optimize their pharmacological and toxicological profile (i.e. minimize cytotoxicity to living cells while retaining DNA-binding capacity) and therefore be used to generate NABNP formulations, such as those based on the PAMAM-G3-$C12_5$-$DEEA_{20}$ and PAMAM-G3-$Cholesterol_5$ backbones, that are able to efficiently scavenge cfDNA *in vivo*, and thus prevent its accumulation in the bloodstream of tumor-bearing animals (accumulation that is secondary to both tumor progression and tumor killing by cytotoxic chemotherapy); and 2) that prevention of cfDNA accumulation in the bloodstream of tumor-bearing animals is able to prevent systemic inflammation (i.e., able to prevent increases in the serum concentration of powerful pro-inflammatory cytokines, such as IL1β, IL6, TNFα) and, most importantly, prevent metastatic dissemination of cancer cells. These two findings are expected to have a profound impact in the development of new treatment strategies for breast cancer, form both a conceptual and applicative point of view, because: 1) they provide *"proof-of-principle"* for a new conceptual approach in the design of cancer-chemotherapy, which aims at combining cytotoxic agents (aimed at killing cancer cells) with cfDNA scavenging agents (aimed at preventing the pro-metastatic effects of the release into the patient's circulation of cfDNA from cancer cells that are killed by cytotoxic agents); and 2) they provide two viable drug-candidates in terms of the translational application of this novel concept (PAMAM-G3-$C12_5$-$DEEA_{20}$, PAMAM-G3-$Cholesterol_5$), both with safe toxicological profiles in mice.

2) **Development and optimization of experimental models for the study of breast cancer metastasis.** Among the important observations made during this study are also: 1) the observation that lentivirus vectors utilizing the *Cytomegalovirus* (CMV) promoter to drive the expression of fluorescent and/or bioluminescent reporters (e.g. lentivirus vectors based on the pLentiLox3.7 backbone; Addgene #11795) are unsuitable for the genetic engineering of mouse breast cancer cells (e.g., 4T1), as they appear to be rapidly silenced, in a manner similar to what previously observed in mouse ES cells (Meilinger *et al.*, *EMBO Reports*, 10:1259-64, 2009); 2) the observation that lentivirus vectors utilizing the EF1a promoter can be used to obtain stable expression of the same reporters across multiple breast cancer cell lines, both murine (4T1) and human (MDA-MB-231; MDA-MB-468; TM-00089, TM-00096, TM-00098); 3) the observation that, in human breast cancer cell lines (MDA-MB-231, MDA-MB-468), the fluorescent and bio-luminescent signals obtained using lentivirus vectors based on the pHIV-Luc-ZsGreen backbone (Addgene #39196), which encodes ZsGreen and Luc2P, are higher than those obtained using lentivirus vectors based on the pLentiLox3.7 backbone (Addgene #11795), which encodes EGFP and Luc. Taken together, these observations will enable future studies in the field of breast cancer metastasis to proceed in a more rapid and efficient manner, as future investigators will have immediate access to a portfolio of breast cancer cell lines, both human and murine, that have already been genetically engineered to express high and stable levels of both fluorescent and bio-luminescent reporters (please, also refer to Section 6, PRODUCTS).

Impact on other disciplines. The results of the experiments performed with the support of this award have also contributed to advances that are expected to translate to other areas or research, including:

1) **Development of new therapeutic approaches against other forms of cancer.** The scientific advancements that have been achieved as a result of this study provide *"proof-of-principle"*

demonstration for a new therapeutic approach to suppress cancer metastasis, and are foreseen to rapidly translate to **other forms of cancer**, as they appear to be widely generalizable. For example, it is well established that cfDNA tends to accumulate in the bloodstream of cancer patients, irrespective of the specific type of malignancy that affects them. It is also well established that cfDNA causes systemic inflammation and promotes the metastatic dissemination of tumors other than breast cancer, such as pancreatic cancer (Ibtehaj *et al.*, *Molecular Therapy*, 26:1020-1031, 2018). It is therefore expected that the treatment approach developed in this study will display similar efficacy across a large spectrum of malignancies. Furthermore, future investigations on the biology of metastasis in other types of mouse cancer models will benefit from the knowledge generated during this study regarding the most effective means of engineering mouse cancer cells with fluorescent and bio-luminescent reporters (e.g. ZsGreen, Luciferase). Future investigators will learn that, in order to achieve stable expression of such reporters in mouse cancer cells, they will likely need to use lentivirus vectors designed to express the reporters under the transcriptional control of the EF1a promoter (as opposed to the CMV promoter).

2) Development of novel, biocompatible drug nano-carriers with applications across multiple areas of human medicine. We developed a novel, nanoparticle-based drug-delivery system that enables the delivery of high payloads of cytotoxic drugs to tumor tissues and, at the same time, the scavenging of cfDNA from the systemic circulation (a double "push-pull" action). This novel, nanoparticle-based drug-delivery system is able to effectively control tumor growth at primary sites, while concurrently suppressing metastatic dissemination. The "push-pull" idea is simple, but also represents an important conceptual advance in the field of cancer nanomedicine. **Our data provide "proof-of-principle" demonstration of the concept that, in drug-formulations, the "carrier" does not need to be a passive entity (i.e., a mere vector for the therapeutic cargo) but can actively participate to therapeutic effects because of its own pharmaco-dynamic activities**. In this study, we designed nano-carriers that specifically aimed at addressing and enduring paradox: that chemotherapy might exacerbate metastasis. Chemotherapy (or radiotherapy, for that matter) causes massive cell death, and thus the release into the extracellular space of large amounts of cellular contents, which act as *damage-associated molecular pattern* (DAMP) molecules. DAMPs are sensed by immune cells, which initiate an inflammatory cascade, which is intended to act as a host-defense mechanism, but which can also facilitate cancer metastasis. A large fraction of the DAMP molecules released in the systemic circulation following chemotherapy are represented by cell-free nucleic acids (cfDNA/cfRNA) and are negatively charged. As such, they can be bound and sequestered (i.e., "scavenged") by cationic polymers, based on electrostatic interactions. By designing cationic NABNPs that can scavenge pathogenic DAMP molecules, we developed a "bio-active" carrier, which is expected to improve the therapeutic profile of any drug formulation that is used for the treatment of conditions in which suppression of damage-induced inflammatory responses is beneficial (e.g., auto-immune disorders, trauma, sepsis and selective viral infections, such as COVID-19).

Impact on technology transfer. A disclosure reporting on the inventions resulting from this study was submitted to the *Columbia Technology Ventures* (CTV) office, which decided to submit a **provisional patent application** to the *United States Patent and Trademark Office* (USPTO):

U.S. Provisional Application **No. 63/349,492:** *Cationic polymeric nanocarriers to inhibit chemotherapy-induced cancer metastasis and cognitive impairment.*

Impact on society beyond science and technology. Nothing to report.

5. CHANGES/PROBLEMS.

Changes in approach. We decided to add two human *triple-negative breast cancer* (TNBC) cell lines (MDA-MB-231, MDA-MB-468) to the portfolio of experimental models to be screened for possible use in the *in vivo* experiments envisioned under this project, which originally included only a mouse TNBC cell line (4T1) and a collection of *patient-derived xenograft* (PDX) lines established from human TNBCs. We decided to implement this expansion because it would have improved the project's quality and probability of success, without causing a meaningful increase in associated costs, especially when

considering that the two cell lines could be genetically engineered and tested in parallel to 4T1 cells, using the leftovers of previously purchased research reagents. Because we considered this change to represent an improvement upon the previous experimental plan (i.e. an expansion as opposed to a substantial modification) and to have no meaningful impact on the overall budget of the project (i.e. to add no additional costs to the study), we regarded it as *"not significant"* (and sought no prior written approval). We also decided to include *doxorubicin* (DOX) among the drugs whose therapeutic activity we plan to improve by complexing with NABNPs, as envisioned during the *no-cost extension* (NCE) period (please, see also the justification outlined above). These experiments will allow us to test whether our NABNP formulations can be leveraged to improve the therapeutic activity of more than one drug used in cancer chemotherapy, and thus validate the generalizability of our "push-pull" concept.

Problems or delays. In addition to the delays caused by the COVID-19 pandemic during the first two years of the award (2020-2021), which were detailed in the two previous technical reports, we have continued to experience issues with the supply-chain of several research reagents (e.g., delayed shipment and delivery). Of significance is also the poor quality of selected reagents, such as certain antibodies, which caused a significant waste of time (and effort) in the completion of key experiments. This led to our request for a *no-cost extension* (NCE) of the award, as it became necessary to complete some of the tasks envisioned in the project.

Changes that had a significant impact on expenditures. Towards the end of the 3rd year of the award (May 2022), one of post-doctoral fellows working on this project (Dr. William J. Raab) completed his training in our laboratory and left *Columbia University* to pursue professional opportunities in the biotechnological industry. Therefore, as of May 1st, 2021, we did not charge this award for the salary of Dr. William J. Raab. To enable the successful continuation of our studies, we decided to recruit into the project a post-doctoral fellow with extensive experience with the use of both lentivirus vectors and animal cancer models (Dr. Pierangela Palmerini, PhD). It is our opinion that Dr. Palmerini is fully equipped with all the technical expertise required to successfully support the development of this project. We propose to replace Dr. William J. Raab with Dr. Pierangela Palmerini for the remaining duration of the award.

Significant changes in use or care of human subjects, vertebrate animals, biohazards, and/or select agents. Nothing to report.

6. PRODUCTS.

Publications with acknowledgment of the support of this project.

1) Li T., Akinade T.O., Zhou J., Wang H., Tong Q., He S., Rinebold E., Valencia Salazar L.E., Bhansali D., Zhong Y., Ruan J., Du J., Dalerba P. and Leong K.W., *Therapeutic nanocarriers inhibit chemotherapy-induced breast cancer metastasis.* **Advanced Science**, e2203949 (2022)
2) Tu Z.X., Zhu Y.F., Xiao Y.Q., Chen J., Shannon S., Zhang F., Li Z.W., Zhou J., Hu H.Z., Ho Z.C., Gao W.L., Shao D. and Leong K.W., *Scavenging Tumor-Derived Small Extracellular Vesicles by Functionalized 2D Materials to Inhibit Tumor Regrowth and Metastasis Following Radiotherapy.* **Advanced Functional Materials**, 32:2205663 (2022).
3) Tu Z., Zhong Y., Hu H., Shao D., Haag R., Schirner M., Lee J., Sullenger B. and Leong K.W., *Design of therapeutic biomaterials to control inflammation.* **Nature Reviews Materials**, 7:557-574 (2022).
4) Naqvi I., Giroux N., Olson L., Morrison S.A., Llanga T., Akinade T.O., Zhu Y., Zhong Y., Bose S., Arvai S., Abramson K., Chen L., Que L., Kraft B., Shen X., Lee J., Leong K.W., Nair S.K. and Sullenger B. *DAMPs/PAMPs induce monocytic TLR activation and tolerance in COVID-19 patients; nucleic acid binding scavengers can counteract such TLR agonists.* **Biomaterials**, 283:121393 (2022).
5) Cai S.S., Li T., Akinade T.O., Zhu Y. and Leong K.W. *Drug delivery carriers with therapeutic functions.* **Advanced Drug Delivery Reviews**, 176:113884 (2021).
6) Mintz R.L., Lao Y.H., Chi C.W., He S., Li M., Quek C.H., Shao D., Chen B., Han J., Wang S. and Leong K.W., *CRISPR/Cas9-mediated mutagenesis to validate the synergy between PARP1*

inhibition and chemotherapy in BRCA1-mutated breast cancer cells. **Bioengineering & Translational Medicine**, 5:e10152 (2020).

Websites or other internet sites. Nothing to report.

Technologies or techniques. Nothing to report.

Inventions, patent applications, and/or licenses. A provisional patent application has been filed to *United States Patent and Trademark Office* (USPTO):

U.S. Provisional Application **No. 63/349,492**: *Cationic polymeric nanocarriers to inhibit chemotherapy-induced cancer metastasis and cognitive impairment*.

Other Products. Among the important products generated during the three years of the award are key research tools and experimental models, consisting in six (n=6) independent breast cancer cell lines engineered to express high levels of both fluorescent (ZsGreen) and bio-luminescent (Luc2P) reporters. All six cell lines were generated by infection with a lentivirus vector based on the *Human Immunodeficiency Virus* (HIV) genomic backbone, and encoding both ZsGreen and Luc2P under the transcriptional control of the *Eukaryotic Translation Elongation Factor 1 Alpha* (EF1a) promoter (Addgene # 39196). For each of the six lines, following lentivirus infection, cells displaying the highest levels of green fluorescence were isolated by *fluorescence activated cell sorting* (FACS) and used to initiate sub-lines expressing the reporters at 100% purity. The six cell lines are:

1 - **4T1-ZsGreen/Luc2P** - murine (derived from **4T1** cells; ATCC #CRL-2539);
2 - **MDA-MB-231-ZsGreen/Luc2P** - human (derived from **MDA-MB-231** cells; ATCC #HTB-26);
3 - **MDA-MB-468-ZsGreen/Luc2P** - human (derived from **MDA-MB-468** cells; ATCC #HTB-132);
4 - **TM-00089-ZsGreen/Luc2P** - human (derived from **TM-00089** cells; The Jackson Laboratory);
5 - **TM-00096-ZsGreen/Luc2P** - human (derived from **TM-00096** cells; The Jackson Laboratory);
6 - **TM-00098-ZsGreen/Luc2P** - human (derived from **TM-00098** cells; The Jackson Laboratory);

7. PARTICIPANTS & OTHER COLLABORATING ORGANIZATIONS.

Individuals working on the project:

1 - Name: **Kam W. Leong, PhD**
Role: **Principal Investigator (PI)**
Researcher identifier: **n.a.**
Person-months working on the project: **1 person-month**
Contribution to project: Supervision of all aspects of the project.
Funding support: **this award and start-up fund from Columbia University**

2 - Name: **Tianyu Li, PhD**
Role: **Postdoctoral fellow**
Researcher identifier: **n.a.**
Person-months working on the project: **12 person-months**
Contribution to project: Dr. Li worked on the synthesis of a library of PAMAM-G3 derivatives. He led the project after Dr. Wang left.
Funding support: **this award and start-up fund from Columbia University**

3 - Name: **Tolu Akinade, BS**
Role: **MD/PhD student**
Researcher identifier: **n.a.**
Person-months working on the project: **12 person-months**

Contribution to project: Ms. Akinade participated in all aspects of the project and is planning for the mechanistic studies in the coming year
Funding support: **this award and a predoctoral fellowship from the MSTP Program**

4 - Name: **Siyu He, BS**
Role: **PhD student**
Researcher identifier: **n.a.**
Person-months working on the project: **3 person-months**
Contribution to project: Ms. Siyu developed the machine-learning technique to analyze the histological tissues using the algorithms published in the literature.
Funding support: **this award and start-up fund from Columbia University**

Changes in active other support of key personnel:

Principal Investigator (PI): **Kam W. Leong**

Active grants that have been **completed**: none

Pending grants that have been **activated**: none

Other organizations involved as partners. Nothing to report.

8. SPECIAL REPORTING REQUIREMENTS.

This is a **collaborative award**, consisting of two independent grants **(BC180904, BC180904P1).** The present report constitutes a “joint report”, representative of the work conducted in collaboration by the two partnering teams (leading team: Kam W. Leong; partnering team: Piero Dalerba)**.**

9. APPENDICES.

Nothing to report.